Structural analyses of the putative mannosylphosphate transferase, Ktr6p, from *Saccharomyces cerevisiae*

Daniella S. Marks

Department of Biochemistry
McGill University, Montreal

February, 2010

A thesis submitted to McGill University in partial fulfillment of the requirements of the degree of Masters of Science.

To my grandfather, David Marks. I could only wish you could see what I have accomplished. And to Dr. Annette Herscovics, another piece of your puzzle has been solved.

ABSTRACT

The post-translational addition of sugar moieties onto proteins plays an important role in protein folding, secretion, signaling, and is even thought to partake in cell-cell adhesion. In eukaryotes, the biosynthesis of N-glycans begins with the transfer of $Glc_3Man_9GlcNAc_2$ to the amide group of an asparagine situated in the tripeptide Asn-X-Thr(Ser), of a protein. Subsequent removal of three glucoses and one mannose occurs in the Endoplasmic Reticulum. In yeast, those proteins that require further maturation, e.g. those destined to enter the secretory pathway, are sent to the *cis*-Golgi. The core, $Man_8GlcNAc_2$, is then decorated with additional mannoses and mannose-1-phosphates.

The enzyme responsible for the transfer of mannose-1-phosphate in *Saccharomyces cerevisiae* is Ktr6p. It is a member of the *K*re *T*wo *R*elated family of mannosyltransferases: Kre2p. Ktr6p shares 38% sequence identity with Kre2p, suggesting a similar three-dimensional structure. However, greater than 50% of the residues in the Ktr6p putative active site differ from Kre2p, signifying that Ktr6p may have a modified mannosyltransferase function. For these aforementioned reasons, crystallographic studies on this putative mannosylphosphate transferase are pursued. Here, we present the methods employed to obtain the final Ktr6p crystal structure that has been solved, via molecular replacement, to a resolution of 3.11 Å. A detailed discussion analyzing the results obtained ensues.

RÉSUMÉ

La glycosylation des protéines joue un rôle important dans leur repliement, leur sécrétion, dans la signalization cellulaire, et pourrait même participer à l'adhérence entre les cellules. Chez les eucaryotes, la biosynthèse de N-glycanes débute avec le transfert de $Glc_3Man_9GlcNAc_2$ à l'amide d'une asparagine située dans la séquence Asn-X-Thr (Ser). L'élimination de trois glucoses et d`un mannose a ensuite lieu dans le réticulum endoplasmique. Dans le cas de la levure, les protéines qui nécessitent encore plus de maturation, par exemple celles destinées à entrer dans la voie de sécrétion, sont envoyées au *cis*-Golgi. Ensuite, la glycane $Man_8GlcNAc_2$, est ornée de mannoses additionels et de mannose-1-phosphate.

L'enzyme responsable du transfert du mannose-1-phosphate dans *Saccharomyces cerevisiae* est Ktr6p. Il est caractérisé comme étant un membre de la famille des mannosyltransferases liés à la protéine Kre2p (KTR). Ktr6p conserve une identité de séquence de 38% avec Kre2p, suggérant une structure homologue. Toutefois, plus de 50% des résidus présents dans le site actif présumé de Ktr6p diffèrent de Kre2p, suggérant que Ktr6p a une fonction différente. Pour ces raisons, des études cristallographiques sur cette mannosyltransferase présumé sont poursuivies. Ici, nous présentons les méthodes employées pour obtenir la structure finale de Ktr6p à une résolution de 3.11 Å en utilisant la technique de remplacement moléculaire. Une discussion détaillée analysant les résultats obtenus suivra.

Table of Contents

ABSTRACT ..... **i**

RÉSUMÉ ..... **ii**

List of Figures ..... **vi**

List of Tables ..... **viii**

ACKNOWLEDGEMENTS ..... **ix**

CHAPTER I – INTRODUCTION **1**

1.1. Principles of Eukaryotic Glycosylation **1**

1.1.1. Glycosylation Overview 1

1.1.2. N-Glycosylation 1

1.1.3. O-Glycosylation 6

1.1.4. Roles of Glycosylation in *Saccharomyces cerevisiae* 9

1.1.4.1. Glycosylation and Its Involvement in Quality Control 9

1.1.4.2. Direct Influence of Glycosylation on Protein Folding 13

1.1.4.3. All Proteins that are Secreted are Glycosylated 14

1.2. Glycosylation Throughout Evolution **14**

1.2.1. A Comparative Analysis between Yeast and Mammalian Cells 14

1.2.2. Glycosylation in Prokaryotes 17

1.3. Elucidation of the Glycosylation Pathway in Yeast **18**

1.3.1. An Introduction to the Composition of the *S. cerevisiae* Cell Wall 18

1.3.2. A Considerable Number of Enzymes in the Pathway are Homologous to Kre2p 20

1.3.3. The Kre Two Related Proteins 23

1.3.4. Introducing Ktr6p/Mnn6 23

1.3.4.1. Regulation of Ktr6p 28

1.3.5. Extensive Processing in *Saccharomyces cerevisiae* 29

1.3.6. Putative Role of Ktr6p/Mnn6p 32

1.4. Mannosephosphate in Pathogenic Fungal Species 32

1.5. Rationale of the Research 33

CHAPTER II - MATERIALS AND METHODS 34

2.1. Materials 34

2.2. Initial Protein Purification and Crystallization Tests 34

2.2.1. Dynamic Light Scattering (DLS) 34

2.2.2. Crystallization Trials 34

2.3. Development of a New Protein Purification Procedure 35

2.4. The Newly Purified Ktr6p in Crystallization Trials 37

2.4.1. Crystal Optimization 37

2.4.2. Co-Crystallization of Ktr6p with its Donor 37

2.5. Cross-linking Crystals with Glutaraldehyde 37

2.6. Tetra Methyl *Ortho*-Silicate (TMOS) and the *in gel* Crystallization Technique 38

2.7. Small-Angle X-Ray Scattering (SAXS) *ab initio* Three Dimensional Reconstruction 38

2.8. Co-Crystallization Data Collection and Processing 38

2.9. Structure Solving and Refinement 39

CHAPTER III - RESULTS 40

3.1. Disparities between Purification Procedures 40

3.2. Peak B Crystallization and Optimization 44

3.2.1. With Glutaraldehyde 44

3.2.2. With Buffer and Opti-Salt Screens 44

3.2.3. With Tetra Methyl *Ortho*-Silicate 44

3.3. Ktr6p Co-Crystallization with GDP-Mannose and Structure Refinement 46

3.4. SAXS *ab initio* Model of Ktr6p in Solution.....53

3.5. Summary of Results 55

CHAPTER IV - DISCUSSION 56

4.1. The Ktr6p Structure in Relation to Other Transferases.....56

4.2. A Detailed Comparison of Ktr6p and Kre2p 56

4.2.1. A Look into the Putative Active site of Ktr6p 59

CHAPTER V – CONCLUSIONS 66

BIBLIOGRAPHY 67

List of Figures

Figure 1: Synthesis of the lipid-linked oligosaccharide and the transfer onto a nascent polypeptide chain in the ER 4

Figure 2: The N-linked core oligosaccharide 5

Figure 3: Structure of an O-glycan in *S. cerevisiae*. 8

Figure 4: Calnexin/Calreticulin protein folding pathway. 12

Figure 5: Types of yeast and mammalian N-glycans that are synthesized. 16

Figure 6: Composition of the fungal cell wall. 19

Figure 7: General schematic of mannosyltransferases 22

Figure 8: Sequence comparison of the nine members of the KTR family. 25

Figure 9: The proposed reaction scheme as catalyzed by Ktr6p. 27

Figure 10: Elongation and decoration of glycoproteins in S. cerevisiae 30

Figure 11: SDS-PAGE representing various stages of the new purification procedure. ... 41

Figure 12: First purification step on an HA column. 42

Figure 13: Automated Mono-Q GL 10/100. 43

Figure 14: Crystals cultivated in different screens. 45

Figure 15: Diffraction Pattern obtained from a crystal grown in 0.1 M MES pH 6.5, 20% PEG 10000, 5 mM GDP-mannose. 47

Figure 16: Atomic structure of Ktr6p. 50

Figure 17: Stick and cartoon representation of specific Ktr6p residues with their respective 2*F*o-*F*c maps contoured at 1 σ. 52

Figure 18: Relatedness of the Ktr6p crystal structure and the SAXS *ab initio* model. 54

Figure 19: Superposition of Ktr6p and Kre2p. 57

Figure 20: Surface view of Ktr6p. 58

Figure 21: Electrostatics of Ktr6p and Kre2p 60

Figure 22: Amino acids in the active site interacting with GDP-mannose and Mn^{2+} 62

Figure 23: Representation of the β-hairpin in the Kre2p and Ktr6p active site. 63

Figure 24: Localization of the Y^{220}, Y^{214} and R^{130} from Kre2p in respect to the Ktr6p active site 64

List of Tables

Table 1: Suites involved in crystallization screens. 36

Table 2: Dynamic Light Scattering data acquisition table. 40

Table 3: Data collection and refinement statistics for Ktr6p 48

ACKNOWLEDGEMENTS

Above all, I would like to thank Dr. Albert Berghuis for giving me a second chance; for seeing potential, for seeing an opportunity, for being more than kind-hearted. I would like to thank him for having an open door policy, and for creating an exceptionally good and healthy lab environment. Thank you for coffee and lunch.

Thank you to Dr. Emil Pai and Dr. Steve Bryson for being excellent mentors and for demonstrating the utmost sensitivity towards my situation. Thank you for your compassion.

To Dr. Walter Mushynski, who has always been a great mentor, and to whom I could always go to for advice. Thank you for always being there in time of need.

Thanks to all my lab mates, who have become dear friends of mine. Thanks for teaching me and for helping me. For being patient and for being quirky and odd. For Wii nights and ski days, for San Francisco and Toronto. Thank you Magda, Oliver, Brahm, Ahmad, Kun, Pedro, Barry, Dmitry, Jae, Shane, Miriam, Anna, Wayne, Des and Dave.

Thank you to my family, Mom, Dad, Laura and Alexander; for instilling good study skills, for teaching me how to persevere, and for encouraging me to pursue my passion. Thank you to my grandparents for taking me in during CEGEP and undergrad. Thank you to my grandmother for being so understanding.

To my friends, all of whom I laughed and cried with, and have the most wonderful memories with. Thank you Mary, Christina, Erin, Sarah G, Sarah BR, Ahilya, and Jen for being so supportive, and for being the amazing women that you are. Thank you Rhetta for endless hours of conversations, silliness, foosball and crazy adventures. Thank you Christian, for always keeping me on my toes, for believing in me and for being by my side.

Thank you.

CHAPTER I – INTRODUCTION

1.1. Principles of Eukaryotic Glycosylation

1.1.1. Glycosylation Overview

Proteins contain a variety of co- and post-translational modifications that are frequently imperative to their functioning. Alterations such as phosphorylation, methylation, lipoylation and glycosylation can drastically affect the manner in which a protein is structured, as well as its function, localization and expression (Herscovics and Orlean 1993). Glycosylation is the most energy-costly and complex modification. Greater than 50% of all proteins synthesized are glycoproteins (Helenius and Aebi 2004), and this covalent modification requires the use of up to 3% of our genes (Murrell 2004).

Our breadth of knowledge on the subject is due, in thanks, to the excellent model systems yeast has provided us with. Most of the enzymes involved have been characterized and the pathways of protein glycosylation elucidated. Originating in the ER, glycoproteins are shuttled to the Golgi apparatus, where further glycan processing is undertaken to give rise to the final product. The glycans bound to the polypeptide chains provide information with regards to protein folding and sorting, and may also act in cell-to-cell recognition and cell protection (Murrell 2004).

In the following subsections, great care will be taken to enlighten the reader on the subject of glycosylation in *Saccharomyces cerevisiae* including: N- and O-glycosylation, as well as its role in folding and maintaining protein integrity, and finally, its place in evolution.

1.1.2. N-Glycosylation

Polypeptides that are synthesized in the ER are modified by N-glycosylation. In the cytosol, while the ribosome translates messenger RNA (mRNA) into polypeptide chains, those with a signal sequence (5-10 hydrophobic residues) in their N-terminal domain are detected by signal recognition particles (SRPs) that direct

the nascent chain towards the ER (Alberts, Johnson et al. 2002). The SRP binds the signal sequence, temporarily halting translation, in order to bring the polypeptide and ribosome towards the ER, where it binds its corresponding SRP receptor (SRP-R). The guanosine-triphosphate (GTP) of both the SRP and SRP-R is hydrolyzed to guanosine-diphosphate (GDP), stimulating the dissociation of the SRP, and translation resumes (Alberts, Johnson et al. 2002). The emerging polypeptide chain is directed through the ER's translocation channel (Sec61 complex) and into the lumen (Alberts, Johnson et al. 2002).

Simultaneously, the core oligosaccharide is synthesized within the same organelle. The reaction takes place on both the cytosolic and lumenal faces of the ER membrane and is dependent on a lipid intermediate, dolichol-phosphate (Dol-P) (Kukuruzinska, Bergh et al. 1987), which in yeast is composed of 14-18 isoprene units (Lehle, Strahl et al. 2006). Synthesis of the oligosaccharide chain starts in the cytoplasm with the addition of the N-acetylglucosaminephosphate (GlcNAc-P) moiety of uridine-diphosphate (UDP-GlcNAc) to the lipid carrier (Dol-P) to form GlcNAc-PP-Dol (Lehle, Strahl et al. 2006). A second UDP-GlcNAc donor is subsequently incorporated (Lehle, Strahl et al. 2006). Then, five mannose (Man) residues are added (from GDP-mannose), giving rise to $Man_5GlcNAc_2$-PP-Dol (Spiro 2000).

A transmembrane flippase protein (RFT1) is responsible for transferring the Dol-PP-heptasaccharide from the cytosolic side to the lumenal face of the ER membrane (Helenius, Ng et al. 2002). Unlike most conventional flippases, RFT1 is not dependent on the energy supply of ATP (Helenius, Ng et al. 2002). Once in the lumen, Dol-P-Man and dolicholphosphate-glucose (Dol-P-Glc) serve as donors for the glycosyltransferase-catalyzed elongation of the oligosaccharide to its final form of $Glc_3Man_9GlcNAc_2$-PP-Dol (Lehle, Strahl et al. 2006) (Fig. 1).

The first two glucoses are bound to the oligosaccharide via an α-1,3 linkage (Fig. 2) (Spiro 2000). However, it is the α-1,2 bond of the terminal glucose molecule (Burda and Aebi 1998) that is of interest, for it pertains to the addition of the glycan onto the polypeptide chain. This particular residue is recognized by

oligosaccharyltransferase (OST) (Helenius and Aebi 2004). Eight subunits join together to form the OST complex: Ost1p, Ost2p, Wbp1, Swp1, Stt3p (the catalytic subunit), Ost3p/Ost6p, Ost4p, and Ost5p (Lehle, Strahl et al. 2006). Nine proteins are listed, but Ost3p and Ost6p are not present together, either one is at hand depending on the proteins to be glycosylated (Schwarz, Knauer et al. 2005).

Working in conjunction with the Sec61 complex, OST will scan the emerging unfolded polypeptide chain for the specific recognition sequon: Asn-X-Ser/Thr, (N-X-S/T) (Helenius and Aebi 2004), where X can be any residue with the exception of proline (Marshall 1974). The reason for this is straightforward: in order to add the glycan to the nitrogen of the asparagine side chain, the polypeptide must bend and bring the serine or threonine residues into close proximity, thereby increasing the nucleophilicity of the nitrogen (Bause 1983). This is obviously not possible in the presence of proline.

Only 66% of sequons are glycosylated (Apweiler, Hermjakob et al. 1999), as dictated by the environment surrounding the sequon, the availability of dolichol-phosphate and sugar residues, and whether Ost3p or Ost6p is present (Mellquist, Kasturi et al. 1998). The generated glycans, however, still necessitate further processing in order to ensure that the glycoproteins have acquired the appropriate three dimensional structures.

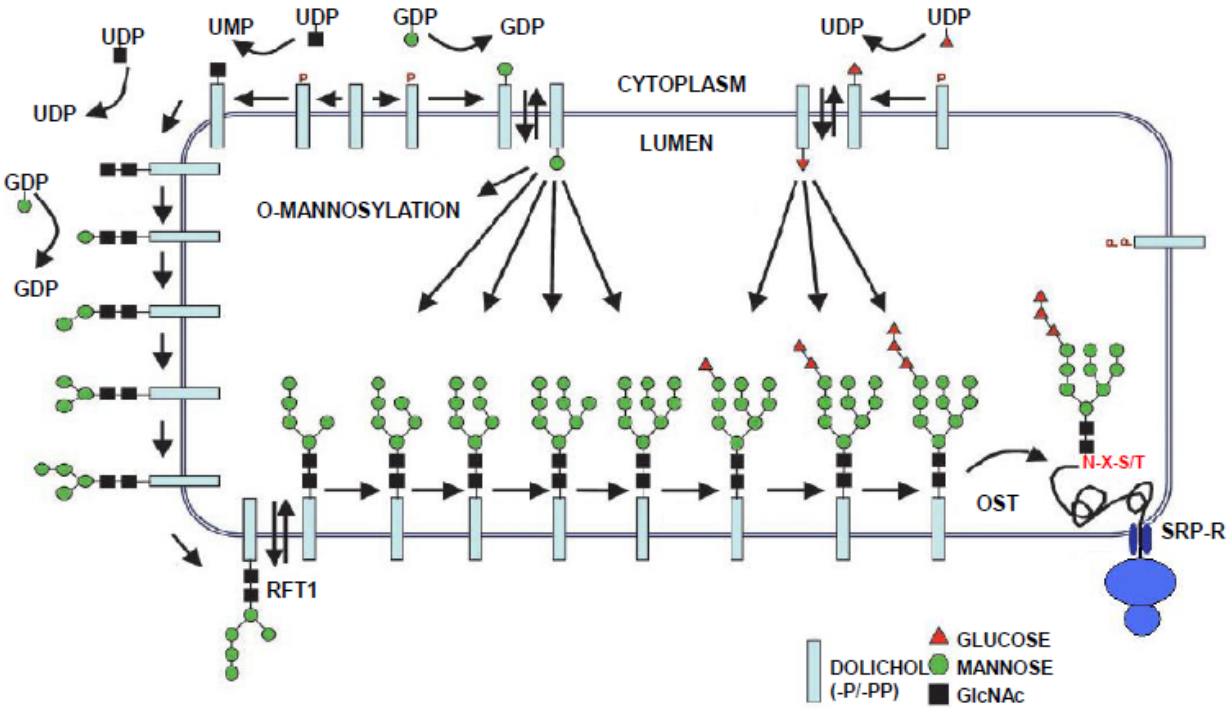

Figure 1: Synthesis of the lipid-linked oligosaccharide and the transfer onto a nascent polypeptide chain in the ER

While the SRP directs the translating protein towards the SRP-R so that it may translocate through Sec61 into the ER, the core oligosaccharide is being assembled. In the cytosol, two GlcNAc and five mannose residues, donated by UDP-GlcNAc and GDP-mannose, are added to the lipid intermediate Dol-P to build $Man_5GlcNAc_2$-PP-Dol. RFT1, a flippase in the membrane, transfers the sugar moiety into the lumen, where Dol-P-mannose and Dol-P-Glucose elongate it to $Glc_3Man_9GlcNAc_2$-PP-Dol. OST recognizes the terminal α-1,2-glucose, as well as the glycosylation sequon N-X-S/T of the nascent polypeptide, and catalyzes the addition of the glycan to the protein.

Adapted from (Helenius and Aebi 2004)

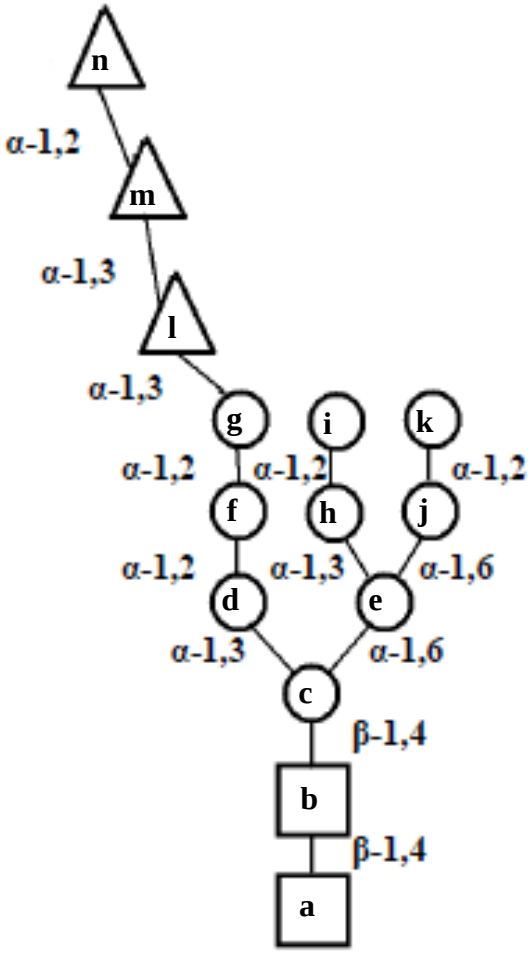

Figure 2: The N-linked core oligosaccharide
The core oligosaccharide consists of three glucoses (triangle), nine mannoses (circle) and two GlcNAc (square). Units labeled a-g are added on the cytosolic face of the ER; h-n, in the lumen. The linkage types are also indicated.
Adapted from (Helenius and Aebi 2004)

1.1.3. O-Glycosylation

Much like its N-linked counterpart, the O-glycan crucially affects protein stability, function and localization. But much less is known about this type of process, and that which is known sheds light on many differences between the two forms of glycosylation. Unlike N-glycosylation, no particular consensus sequence has been identified amongst species; the types of sugars added vary greatly, as does the manner in which they are added to the protein. Where in N-glycosylation the glycan is transferred to the protein *en bloc* by OST, in O-glycosylation, the individual sugar residues are added in a stepwise fashion (Spiro 2002).

In yeast, specifically *Saccharomyces cerevisiae* where O-glycosylation is of the O-mannosylation type, the addition of O-glycan structures has been extensively studied. O-glycosylation involves appending mannosyl moieties, a process mediated by the *p*rotein O-*m*annosyl*t*ransferase (PMT) (Goto 2007). On the whole, it is widely accepted that there are seven members of the PMT family, all of which share conserved transmembrane domains (Type III) (Strahl-Bolsinger and Scheinost 1999). Despite a significant degree of similarity (57.5%) (Goto 2007), they exhibit specificity for acceptor proteins, depending on the PMT complex that is formed (Gentzsch and Tanner 1996). Sequential mutations of the *PMT* genes do not result in lethality or affect the length of the glycans, as would be anticipated, rather they reduce the actual number of glycans added to the protein structure as compared to the wild type (Goto 2007). Generally, it is concluded that O-mannosylation catalyzed by PMT plays a significant role in maintaining cell wall structure and stability.

Contrary to N-glycosylation, in which the first sugar residues are donated by nucleotide sugars, the initiation of O-glycosylation in *S. cerevisiae* requires that the dolichol-phosphate, in the form of Dol-P-mannose, serves as a sugar donor (Strahl-Bolsinger, Gentzsch et al. 1999). The mannose, through the action of the PMT family, is transferred to the β-hydroxyl of either a serine or threonine of a protein in the ER (Gentzsch and Tanner 1997). Following transfer to the Golgi apparatus, an α-1,2-mannosyltransferase (Kre2p) uses GDP-mannose as a donor

to add two sugars to the elongating glycan chain (Lussier, Sdicu et al. 1997). Lastly, three isoenzymes of an α-1,3-mannosyltransferase (*Sc*Mnn1p, *Sc*Mnt2p, *Sc*Mnt3p) are involved in adding the fourth and fifth sugar groups (Goto 2007). All three enzymes collaborate to add the fourth mannose, and *Sc*Mnt2p affixes the terminal sugar (Goto 2007) (Fig. 3).

Although no specific motif has been identified, it has been observed that regions concentrated with serine/threonine (25-40% of the sequence) serve as reasonably good acceptors (Jentoft 1990). What is interesting to note is that these same regions, which are normally prone to digestion by proteases, are now protected by the carbohydrate structure.

The presence of the mannose-chain bound to proteins on the cell membrane is thought to regulate interactions with neighbouring cells. Studies varying the amount of glycoproteins on the cell surface have distinct effects on antigen accessibility (Jentoft 1990). Since the glycan extends relatively far above the surface, it may also serve as a recognition tool (Jentoft 1990).

As mentioned above, other forms of O-glycosylation exist and involve the addition of a variety of sugars including GlcNAc (mucins), fucose (epidermal growth factor), and xylose (heparan sulphate glycosaminoglycan), to name a few (Spiro 2002). The diversity in substrates and in function is complex, and yet, O-glycosylation has been maintained throughout evolution.

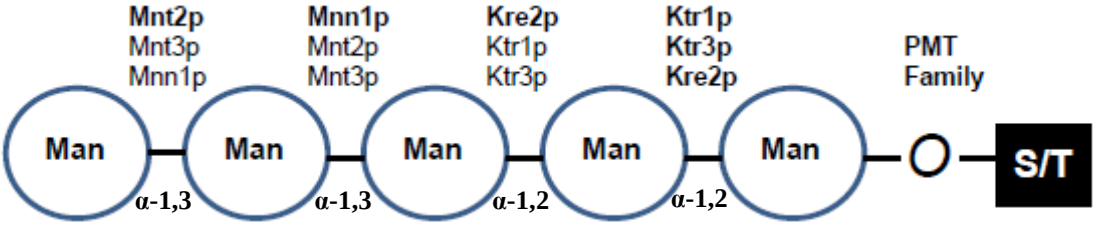

Figure 3: Structure of an O-glycan in *S. cerevisiae*.
The stepwise addition of up to five mannose residues is characteristic of O-mannosylation. A particular consensus sequence has yet to be identified, however, a trend indicates that regions concentrated in serine or threonine residues tend to be favoured. The PMT family catalyzes the addition of the primary mannose from Dol-P-mannose to the protein in the ER. Once brought to the Golgi, Kre2p, an α-1,2-mannosyltransferase, utilizes GDP-mannose to add the second and third sugar. Finally, three isoenzymes collaborate to affix the fourth and fifth mannose. The major enzymes catalyzing each reaction are shown in bold, as well as the linkages between each sugar residue.

(Romero, Lussier et al. 1999)

1.1.4. Roles of Glycosylation in *Saccharomyces cerevisiae*

Notwithstanding that glycosylation is one of the most prevalent forms of post-translational modifications, its function remains enigmatic. It has been put forth that glycosylation fulfills intracellular (protein folding and sorting) and intercellular (immune response and cell-cell recognition) roles (Lehle, Strahl et al. 2006). If an enzyme involved in the glycosylation pathway is defective, the synthesized N-glycoproteins may be unstable, less active, or deficient in the number of polysaccharides attached. The resulting effects can vary, depending on the affected enzyme, but a complete incapability of synthesizing glycoproteins results in lethality (Goto 2007).

1.1.4.1. Glycosylation and Its Involvement in Quality Control

Amongst its multifarious activities, the N-glycan chains serve as sorting signals to distinguish between properly folded and unfolded proteins in the ER. This "glycan processing" pathway encompasses a variety of tools to ensure that only the folded protein leaves the ER to fulfill its destiny. Misfolded proteins, on the other hand, are subject to protein degradation in the cytosol.

This quality control mechanism is cyclic in nature, and aims to refold proteins until they have attained their native structure. It is mediated by two molecular chaperones, Calnexin (CNX) and Calreticulin (CRT). The former is a Type I transmembrane protein and the latter is a soluble protein; both are calcium-dependent (Helenius and Aebi 2004). Their roles in the initial recognition of the glycosylated protein are imperative. As the nascent protein is translocated into the ER and glycosylated by OST, the core glycan is immediately recognized by glucosidase I (Helenius and Aebi 2004), a Type II membrane protein. It removes the glucose residue that has an α-1,2 linkage (highlighted as "n" in Fig. 2) (Herscovics and Orlean 1993). Likewise, glucosidase II removes the middle glucose molecule (denoted as "m" in Fig. 2) (Herscovics and Orlean 1993). Both enzymes together cause dissociation of the glycoprotein from OST and prepare it for entry into the calnexin/calreticulin cycle (Helenius and Aebi 2004). CNX

and/or CRT appropriate the now mono-glucosylated protein and present it to ERp57, a thiol-disulfide oxidoreductase (Maattanen, Kozlov et al. 2006) responsible for the generation of disulfide bridges specifically in glycoproteins, to ensure that the final folded structure is reached (Denisov, Maattanen et al. 2009). Glucosidase II then removes the final glucose moiety and the protein is released from CNX/CRT (Helenius and Aebi 2004). If folded correctly, the protein exits the ER (Fig. 4).

In the situation where the protein is misfolded, UDP-Glucose Glycoprotein Glucosyltransferase (UGGT) becomes involved and transfers a glucose residue from UDP-glucose onto the glycoprotein (Parodi 2000). Many hypotheses have been presented concerning how exactly UGGT "senses" misfolding: the more accepted one being that it is very sensitive to the appearance of hydrophobic patches that unfolded proteins generally seem to have, and in such a case, UGGT will reglucosylate those glycans in the misfolded regions to form $Glc_1Man_9NAcGlc_2$ (Helenius and Aebi 2004). Consequently, the glycoprotein can rebind CNX/CRT, and the cycle recommences with the aspiration that protein will now properly refold and can then be released.

It does occur however, that the protein never refolds correctly, and to avoid accumulation of these improperly folded proteins, they must be degraded by the ER-associated degradation pathway (ERAD) (Kostova and Wolf 2003). It has been shown that this process is time-dependent. Only those proteins that appear to be misfolded and that linger in the ER between 30-90 minutes are subject to degradation (Lippincott-Schwartz, Bonifacino et al. 1988). Proteins that are destined to remain in the ER may very well avoid this fate due to the presence of a folding sensor (Helenius and Aebi 2004). Hence, both time and conformation play a role.

The terminally unfolded protein is recognized by an ER degradation enhancing-mannosidase-like protein (EDEM), stimulating the retrotranslocation of the glycoprotein to the cytosol through the Sec61 channel, so that it enters the ERAD pathway. The glycoprotein is modified by a poly-ubiquitin chain, targeting it to

the proteosome (Schrader, Harstad et al. 2009), so that it will be proteolytically cleaved and no longer present itself as a burden on the cell.

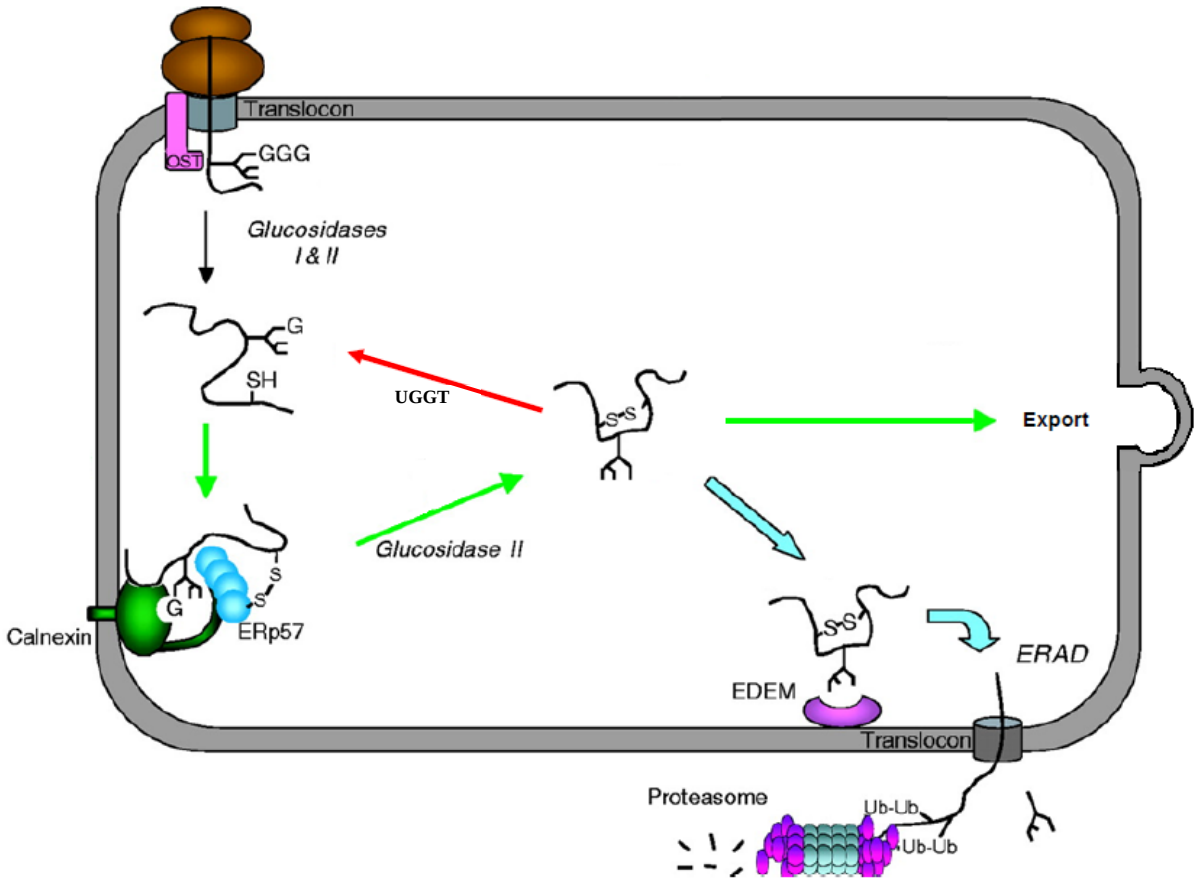

Figure 4: Calnexin/Calreticulin protein folding pathway.
Prior to its release from the ER, the fold of the glycoprotein must be assessed. Glucosidase I and II remove the terminal glucoses, causing the release of the polypeptide from OST. Calnexin and/or the soluble calreticulin appropriate the mono-glucosylated protein, and present it to ERp57, which will generate the disulfide bridges. Glucosidase II removes the last glucose residue, and if folded correctly, the protein is released from the ER (green arrows). However, if the proper tertiary structure has not been attained, glucosyltransferase (UGGT) transfers a glucose monomer from UDP-glucose in order to return it to the calnexin/calreticulin cycle, with the aspiration that the protein will refold (red arrow). Finally, if the protein is terminally unfolded, the non-glucosylated form of the glycoprotein is recognized by EDEM and retrotranslocated through Sec61 into the cytosol, to follow the ERAD pathway, where it will be poly-ubiquitinated and proteolytically degraded (cyan arrows).

Adapted from (Williams 2006)

1.1.4.2. Direct Influence of Glycosylation on Protein Folding

The addition of a polysaccharide chain to a protein drastically affects the protein's biophysical properties. The carbohydrate moieties are large, polar molecules that normally extend far above the surface of the protein and may act in increasing its solubility (Shental-Bechor and Levy 2009) and provide protection against proteolysis (Jentoft 1990). Also, the multiple possible combinations of sugar arrays delineate specificity and generate a diversity that reaches beyond that which is dictated by the primary sequence (Spiro 2002).

Although experimental studies on the effect of glycosylation on protein folding are seriously lacking, a few groups have attempted to decipher this query through *in silico* means (Shental-Bechor and Levy 2008). A bead model of an SH3 domain was constructed: despite it itself not being glycosylated, its protein folding pattern is known and the studied glycosylation sites were engineered *in silico* (Shental-Bechor and Levy 2008). The Levy group then observed the effects of glycosylation by altering the following factors: the length of the polysaccharide chain and the number of sites glycosylated (Shental-Bechor and Levy 2008).

Traditionally, it is hypothesized that proteins are funneled through a folding path that encounters many energy landscapes until it finds the one that is the most energetically favourable (Shental-Bechor and Levy 2009). The simulations performed examined the free energy difference (between the unfolded and folded states) of the glycosylated proteins as compared to the non-glycosylated form (Shental-Bechor and Levy 2008). It was revealed that the energy difference is greater in glycosylated proteins, making them more thermodynamically stable (Shental-Bechor and Levy 2008). What is curious is that this enhanced thermostability may be conferred by the destabilization of the unfolded protein: both the enthalpy and entropy increase, suggesting that the carbohydrates induce a pressure on the protein's conformation (Shental-Bechor and Levy 2009). Whilst these enthalpic and entropic effects are important, there is something to be said about the position of glycosylation: some sites may be crucial for folding, others may not (Shental-Bechor and Levy 2008). It can also be said that glycosylation

not only aids in folding by restricting the paths that a protein may follow, but as a consequence, it may in the end also speed up the reaction process (Liu, Borgert et al. 2008).

1.1.4.3. All Proteins that are Secreted are Glycosylated

It is a well known fact that those proteins destined to be secreted to the cell surface must first be glycosylated as a means to ensure proper conformation and biological activity (Helenius and Aebi 2004) (for example, invertase hydrolyzes sucrose (Delgado, Gil et al. 2003)). Once verified that the protein is indeed functional, it is believed that secretion, in *S. cerevisiae*, then occurs through a constitutive pathway: proteins are secreted immediately to the periplasm, regardless of the environmental stimulus. This differs from the regulated form of secretion where proteins are stored in granules, and their release is dependent on external factors (Walworth and Novick 1987).

Once expelled into the periplasmic space, the glycoproteins form the underlying basis of the cell wall, protecting and supporting the yeast cell itself (Lesage and Bussey 2006).

1.2. Glycosylation Throughout Evolution

1.2.1. A Comparative Analysis between Yeast and Mammalian Cells

The simple fact that N- and O-glycosylation, as a whole, have been so stringently conserved in eukaryotic species is an authentication of their significance. Intensive studies have revealed that across an array of eukaryotic kingdoms, the pathways and enzymes involved in this post-translational modification are homologous. Only few differences exist.

What proved most interesting to researchers was the discovery that in both higher and lower eukaryotes, dolichol sugars are imperative to the reaction mechanism (Gentzsch and Tanner 1996). This indicates that similarities exist between humans and yeast in terms of how the carbohydrates are transferred to the proteins. And while most proteins in the pathway are conserved, including the core molecule,

one of the main differences that exists originates in the composition of OST. Whereas in yeast, OST is composed of nine subunits, in mammals, only seven have been identified: they are lacking Ost4 and Ost5 (Lehle, Strahl et al. 2006). Additionally, the OST complex in yeast consists of one form of Stt3, whereas in mammalian cells, the presence of one of two OST complexes containing isoforms of the Stt3 subunit exerts specific enzymatic properties depending on the tissue in which it is expressed (Lehle, Strahl et al. 2006). In O-glycosylation, a similar disparity occurs in the context of the PMT family: yeast contain seven subfamilies, but higher eukaryotes only contain PMT2 and PMT4, which consequently may affect the number of carbohydrate chains added to the protein (Lehle, Strahl et al. 2006).

In terms of the types of polysaccharide chains that can be made, higher eukaryotes can synthesize three types of glycan structures: high mannose, complex and hybrid chains (Varki, Cummings et al. 1999). In the first case, the core oligosaccharide is modified to $Man_{5-9}GlcNAc_2$ in the ER. In the Golgi, complex chains are synthesized, where the α-1,3- and α-1,6-linked mannose residues are substituted with GlcNAc, and where galactose and sialic acid are also incorporated (Voet and Voet 2004). Finally, hybrid chains can be produced, in which case components of both high-mannose and complex chains are integrated (Fig. 5) (Voet and Voet 2004). In yeast, two types of glycans exist: the core-type ($Man_{8-13}GlcNAc_2$) and the mannan outer chain type, where 100-300 mannose residues elongate the core (Fig. 5) (Jigami 2008).

Indeed, the conservation is so great throughout evolution that it has enabled scientists to study human diseases associated with N-glycosylation in yeast, even to the point of identifying the genes likely to be defective in humans (Jigami 2008).

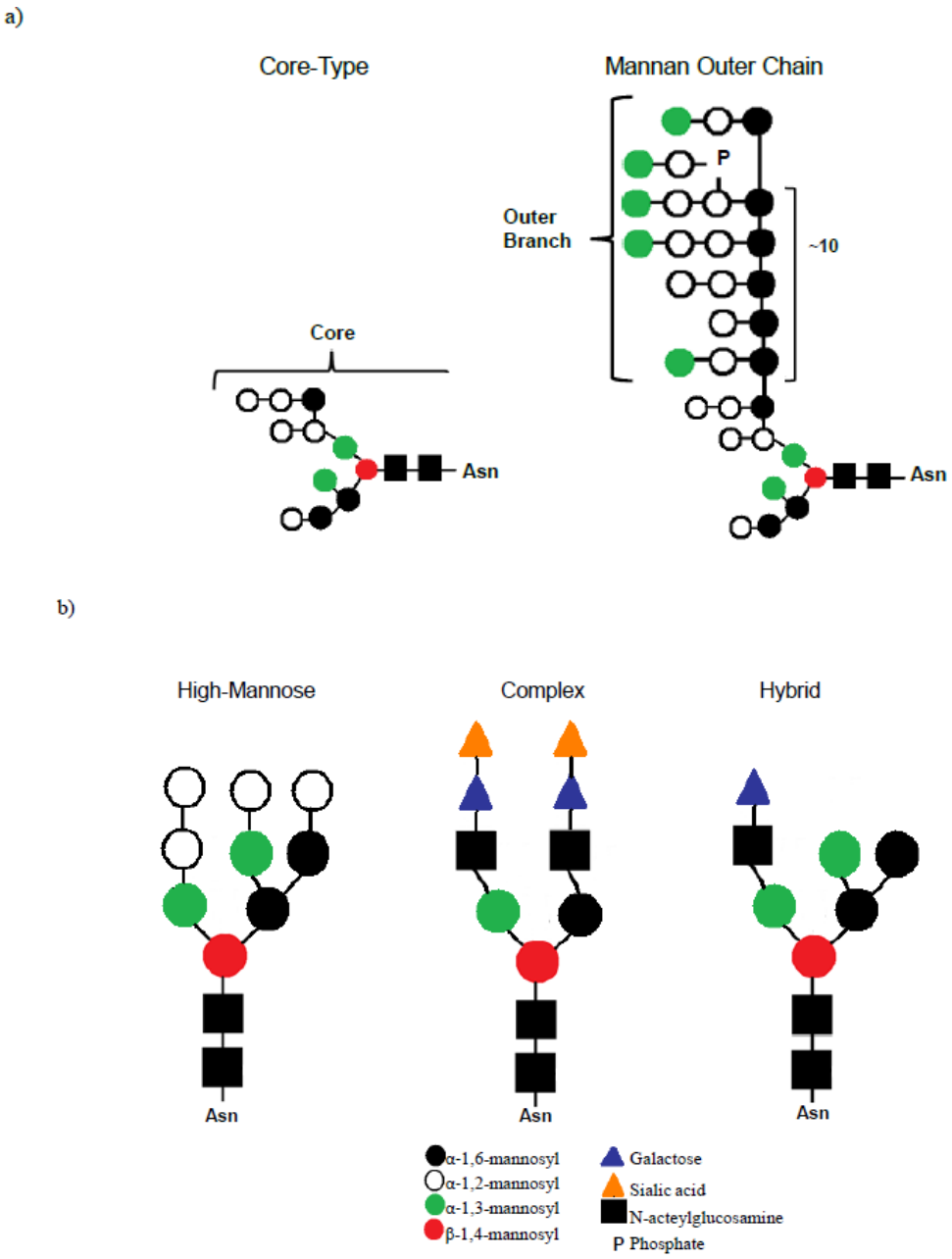

Figure 5: Types of yeast and mammalian N-glycans that are synthesized.
a) In yeast, there are two main types of N-glycans that are produced in the Golgi: the core type and the mannan outer chain type. For the former, very few mannose residues are added to the core oligosaccharide. In contrast, for the mannan outer chain type, 100-300 mannose residues may be incorporated, as well as mannose-1-phosphate (Munro 2001). b) In mammalian cells, high-mannose chains are formed in the ER ($Man_{5-9}GlcNAc_2$). In the Golgi, complex chains (consisting of varying amounts of GlcNAc, galactose and sialic acid) and hybrid glycans (combining properties of high-mannose and complex chains) exist (Voet and Voet 2004).

1.2.2. Glycosylation in Prokaryotes

Om P. Bahl declared in 1992 that "bacteria, in general, do not contain glycoproteins" (Messner 2009). Since then, multitudes of examples of glycosylation have arisen in prokaryotes: in bacteria as well as in archaea. The first case to be discovered, from non-pathogenic bacteria, were the surface-layer (S-layer) glycoproteins that can either be N- or O-glycosylated (Messner 2004). In archaea, these are, more often than not, N-glycosylated (Abu-Qarn, Eichler et al. 2008).

More interestingly, it has been found that pili and flagella, of both kingdoms, are also heavily glycosylated; a characteristic that can be exploited when studying prokaryotic species (Abu-Qarn, Eichler et al. 2008). For example, *Campylobacter coli's* primary flagella component, flagellin, is subject to O-glycosylation, and when disrupted, the filament can no longer assemble, thereby impeding the flagella's motility and invasive properties (Messner 2004). In *Campylobacter jejuni*, disassembling its extensive N-glycosylation system results in the attenuation of ferret diarrheal disease (Goon, Ewing et al. 2006). In the case of another Gram-negative species, *Neisseria gonorrhoeae*, the protein pilin is bound to an O-glycan, and it is postulated that it might play a role in protein folding (Abu-Qarn, Eichler et al. 2008).

Although there does seem to be a fair degree of conservation, differences do exist between eukaryotic and prokaryotic glycosylation systems. As previously mentioned, where the eukaryotic N-glycosylation sequence is N-X-S/T, in prokaryotes, it is D/E-Z-N-X-S/T (X and Z are any amino acid with the exception of proline) (Abu-Qarn, Eichler et al. 2008). However, it is the kinds of monosaccharides that are incorporated into the glycans that greatly separate the two groups: eukaryotic glycans consists mostly of glucose and N-acetylgalactosamine, and in prokaryotes, the glycans are composed of rare sugars such as pseudaminic acid and legionaminic acid (Abu-Qarn, Eichler et al. 2008).

The boom in research, over the past twenty years, in a field that was once thought improbable and unimportant, is remarkable. It has led to many significant discoveries, not only in terms of scientifically outlining new phenomena, but also in perhaps providing an alternate target among pathogenic strains.

1.3. Elucidation of the Glycosylation Pathway in Yeast

1.3.1. An Introduction to the Composition of the *S. cerevisiae* Cell Wall

For the most part, the underlying systems of fungal species, i.e. the secretory pathway, are conserved. The cell wall, on the other hand, differs substantially between species, an attestation to the fact that evolutionary diversity may stem from this structural component (Lesage and Bussey 2006). By virtue of its location and its highly dynamic nature, the cell wall not only serves as a protective barrier, but is also responsible for interactions occurring between itself and its host, (be it receptor-mediated or through adherence), porosity and virulence (Chaffin 2008).

The cell wall accounts for 30% of the cell's dry weight; it consists of 85% polysaccharides (glucose, GlcNAc, mannose) and 15% proteins (Harris, Mora-Montes et al. 2009). The sugar residues can be linked together to form higher level cell wall structures: β-1,3-glucan chains, which are microfibrillar in nature, confer elasticity to the cell wall; the chitin polymer forms hydrogen bonds with neighbouring polymers to increase the strength of the matrix; β-1,6-glucan is capable of cross-linking the two aforementioned polymer structures to mannoproteins (Lesage and Bussey 2006). All the cross-linking, the generation of a fibrillar network, as well as the glycoproteins positioned in the cell wall via a GPI-anchor (Chaffin 2008) result in the collective formation of yeast mannan (Lesage and Bussey 2006) (Fig. 6).

In short, there are glycoproteins that directly affect cell wall composition (e.g. chitin synthase), whereas others act in the extracellular space (e.g. pheromones responsible for mating) (Chaffin 2008). However, prior to their secretion, these proteins must be further processed through a complex pathway specific to yeast, which is outlined in detail below.

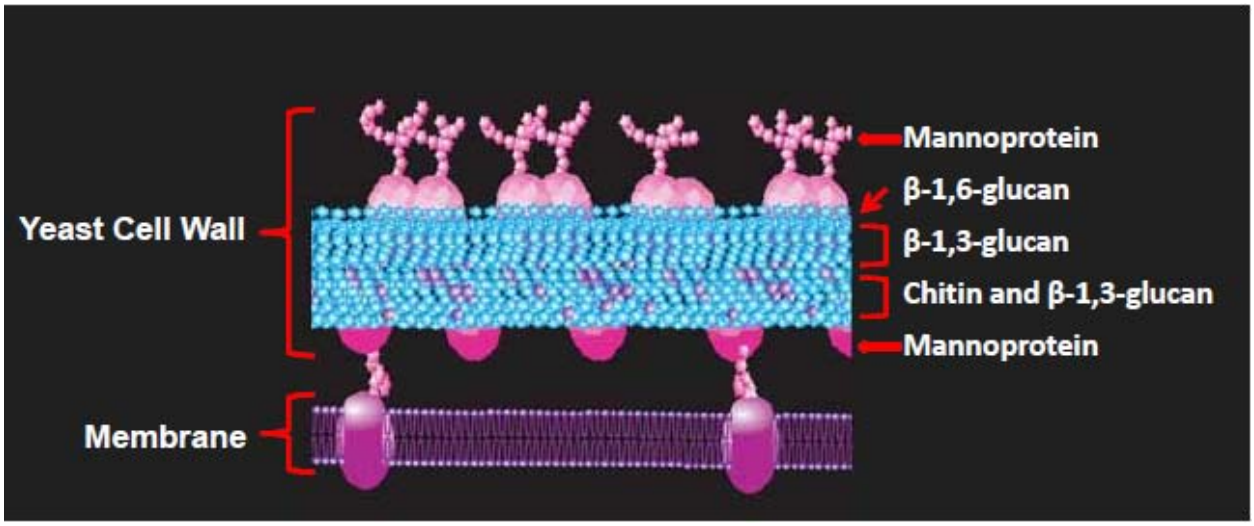

Figure 6: Composition of the fungal cell wall.
The cell wall confers diversity among fungal species in addition to its protective role. 85% of its composition is imparted by the presence of polysaccharides, which can be linked to form higher level structures. β-1,3-glucan chains bestow elasticity, whereas chitin maximizes the cell wall's strength, and the cross-linking between these two structures to mannoproteins results in the formation of β-1,6-glucan. The entire network is referred to as mannan.

Adapted from (Sigma-Aldrich)

1.3.2. A Considerable Number of Enzymes in the Pathway are Homologous to Kre2p

Before divulging the extensive mechanism of yeast glycoprotein modification, a detailed introduction to a few of the protein families will be presented. In yeast, glycoproteins synthesized in the ER are shuttled to the Golgi, where the core is presented with one of two fates: firstly, an exquisitely long outer mannose chain can be added, or, it can be matured into Man_{8}-$_{13}GlcNac_{2}$ (Lussier, Sdicu et al. 1999). In the former situation, many of the proteins involved in elongating, branching, and decorating the core $Man_{8}GlcNAc_{2}$ belong to the *K*re *T*wo *R*elated (KTR) protein group (Lussier, Sdicu et al. 1999). As its name suggests, the members of this family are homologous to the protein Kre2p (*K*iller Toxin *Re*lated protein) (Lussier, Sdicu et al. 1999).

Kre2p functions as an α-1,2-mannosyltransferase, and interestingly enough, it is involved in both N- and O-outer chain glycosylation (Lobsanov, Romero et al. 2004). In the case of the earlier modification type, it catalyzes the creation of an α-1,2-mannose branch that extends from the α-1,6-mannose outer chain (Lobsanov, Romero et al. 2004). This manganese-dependent reaction utilizes GDP-mannose for a donor and an acceptor such as α-methylmannoside (Lussier, Sdicu et al. 1999). As mentioned previously, when Kre2p behaves as an O-mannosylation enzyme, it adds the second and third sugars in the mannose chain that is composed of up to five mannose residues.

Like many of the proteins to be discussed, it is a Type II transmembrane protein, whose N-terminal domain faces the cytoplasm and its catalytic C-terminal tail is positioned in the lumen (Lussier, Sdicu et al. 1999). A soluble construct consisting solely of the lumenal region still maintains catalytic activity, thus facilitating structural analyses (Lobsanov, Romero et al. 2004). With the solving of its structure, it was revealed that it is part of the glycosyltransferase-A family 15 (GT-A 15). This family is characterized by encompassing a single mixed α-β Rossmann fold (Lobsanov, Romero et al. 2004), a motif that is imperative for all nucleotide-binding proteins, as well as a DXD motif variant, important in

coordinating the nucleotide-sugar and the manganese (Fig. 7). Moreover, the members of the KTR family are retaining glycosyltransferases, where prior to, and after the addition of the acceptor, the sugar residue maintains its anomeric conformation (Persson, Ly et al. 2001).

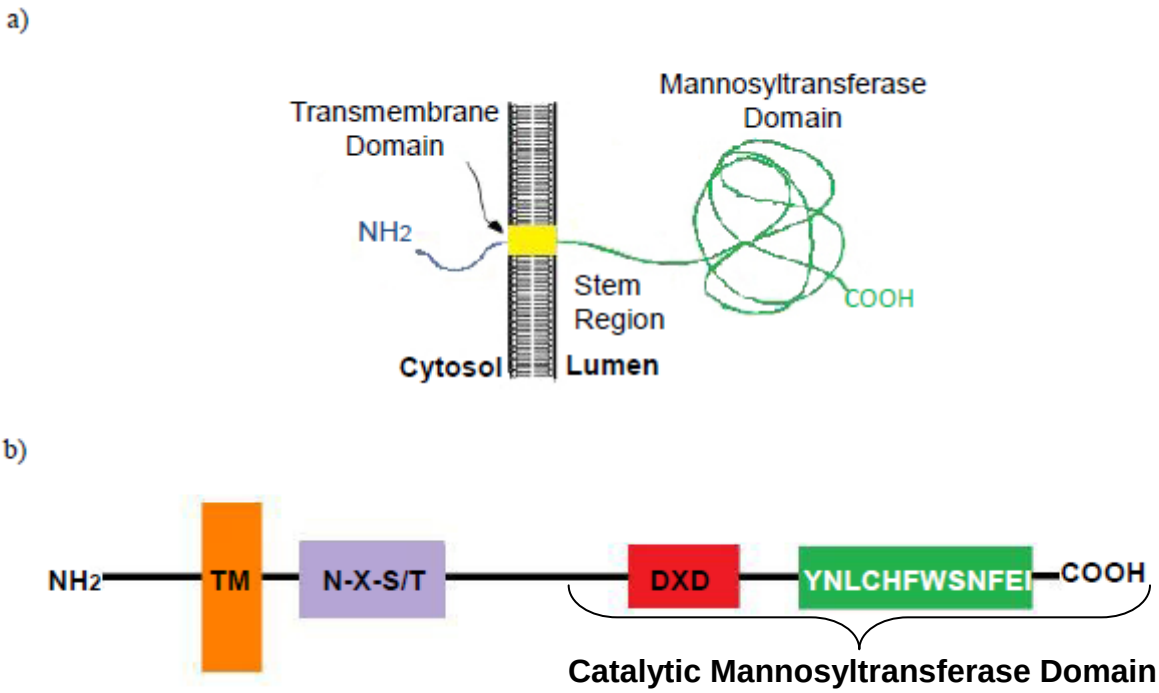

Figure 7: General schematic of mannosyltransferases.
a) Mannosyltransferases, including Kre2p and Ktr6p share a homologous Type II membrane structure, where the mannosyltransferase domain can be cleaved *in vitro* and still retain enzymatic activity (Lussier 1999). b) With the exception of Ktr3p and Ktr4p, mannosyltransferases contain at least one putative glycosylation site in their stem region. The DXD motif is imperative for coordination of the manganese and the GDP-mannose. Finally, the catalytic region includes a relatively conserved sequence that may be indicative of the active site. Additionally, the mannosyltransferase domain adopts a mixed α-β Rossmann fold.

Mutants resistant to K1 killer toxin aided in the elucidation of the glycoprotein pathway. Normally, the toxin binds to the glycans present on a cell surface receptor, and, in a receptor-dependent fashion, leads to the formation of pores conferring lethality to the cells (Hill, Boone et al. 1992). However, those mutants that demonstrated resistance revealed that the receptors differed in terms of their glycan composition as compared to the wild type. These differences allowed for researchers to outline the steps involved in their synthesis. *kre2*-null mutants had shorter mannose chains, resulting in less glycan-mannoprotein cross-linking and affecting the major component of the cell wall (Hill, Boone et al. 1992). Consequently, the K1 killer toxin could not bind, and resistance ensued. This suggested that Kre2p was responsible for modifying proteins on the cell surface (Hill, Boone et al. 1992).

1.3.3. The Kre Two Related Proteins

Alongside the killer toxin resistant screen, and with the sequencing of the yeast genome completed, multiple proteins have been identified that show great similarity to Kre2p. As such, the nine members identified have appropriately been classified under the *K*re *T*wo *R*elated protein family (KTR): Kre2p, Yur1p, Ktr1p, Ktr2p, Ktr3p, Ktr4p, Ktr5p, Ktr6p and Ktr7p (Lussier, Sdicu et al. 1999). Many of the genes in this family were discovered through mutational studies, and are otherwise referred to as *MNN* genes (*mann*osyltransferase-i.e. Ktr6p/Mnn6).

Consistent with the general topology of Kre2p, the KTR proteins are also delineated as having four categorized domains: the cytoplasmic N-terminus, the transmembrane section, the stem region, and the catalytic C-terminal domain (the latter two are present in the lumen) (Lobsanov, Romero et al. 2004). Additionally, each protein, with the exception of Ktr3p and Ktr4p, is predicted to contain at least one glycosylation site in its lumenal domain (Fig. 7) (Lussier, Sdicu et al. 1999).

1.3.4. Introducing Ktr6p/Mnn6

For the most part, the catalytic domain, otherwise known as the mannosyltransferase domain, is well conserved amongst the members of the KTR

family. Sequence alignments reveal that each protein contains six cysteine residues that are conserved in a similar location (Lussier, Sdicu et al. 1999). However, when comparing the proteins as a whole, the sequence similarity is less significant, with Ktr6p demonstrating the least similarity to the members of its family (38% sequence identity with Kre2p) (Wang, Nakayama et al. 1997) (Fig. 8). The catalytic domain of the KTR proteins is of particular interest and with the exception of Ktr6p, each member possesses a conserved sequence located in the distal region of the C-terminus: **YNLCHFWSNFEI** (Lussier, Sdicu et al. 1999). This could lead one to postulate that this is a component of the active site in the mannosyltransferase domain (Lussier, Sdicu et al. 1999). The sequence found in Ktr6p is shown as follows: **FNNCEFTSNFEI** (Lussier, Sdicu et al. 1999). The significant variance in amino acid composition leads to the reasoning that Ktr6p may indeed play a different role in the transfer of a mannose moiety, and this is consistent with the fact that it is believed to be a mannosylphosphate transferase.

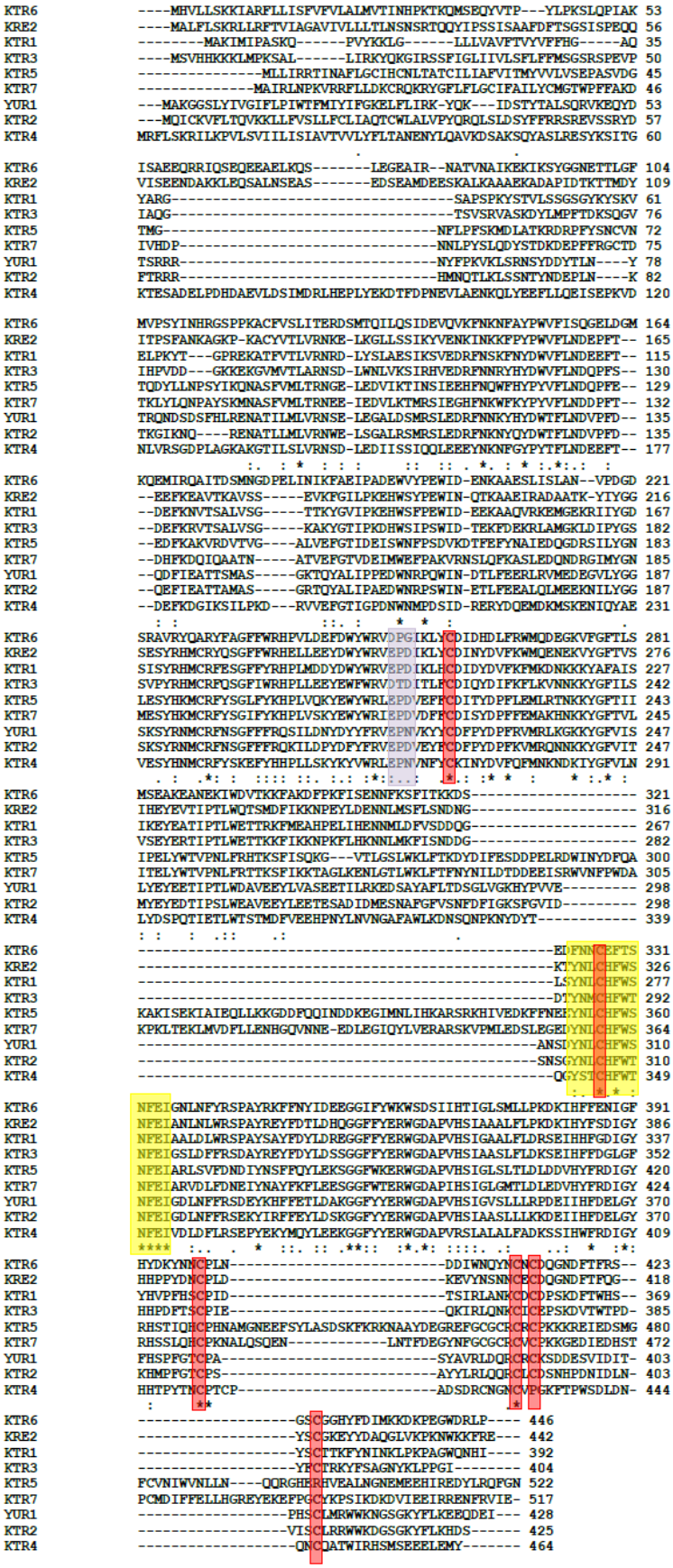

Figure 8: Sequence comparison of the nine members of the KTR family. The amino acids, denoted in single-letter code, are aligned so as to emphasize similarities existing between family members. In red, the conserved cysteines are highlighted; in yellow, the putative active site; and in purple, the DXD motif variant, (DPG in Ktr6p).

The *KTR6* gene was identified through mutational studies involving Alcian blue binding assays, a dye that binds negatively charged macromolecules and stains them blue (Wang, Nakayama et al. 1997). Hence, cells that are deficient in the protein are stained white. When screened against a variety of compounds, the *ktr6*-null mutant exhibited reduced mannosylphosphate transferase activity, suggesting that the gene is involved in mannosylphosphate transfer (Karson and Ballou 1978). It has also been demonstrated that it is not essential for survival in *S. cerevisiae* (Wang, Nakayama et al. 1997). Furthermore, *ktr6* mutants show high sensitivity towards calcofluor white (CFW) and hygromycin B. CFW intercalates between cell surface molecules and allows the aminoglycoside antibiotic to penetrate, (Lussier, Sdicu et al. 1999), meaning that the *KTR6* gene is indeed involved in modifying the cell surface, and may play a role in porosity (Jigami and Odani 1999).

The precise mechanism of action of the 446 amino acid protein, Ktr6p, remains to be solved (Wang, Nakayama et al. 1997). The original mutational studies revealed that Ktr6p acts on the outer branch of N-linked glycans or on O-linked oligosaccharides (Jigami and Odani 1999). However, phosphorylation may not be exclusive to the outer chain. In a transferase assay, where GDP-mannose is the donor and a core molecule acts as the acceptor, the activity of the mutant diminished with respect to the wild type, signifying its role in core-oligosaccharide phosphorylation (Wang, Nakayama et al. 1997). In fact, four positions have been identified as being putative mannose-1-phosphate transfer sites: two in the outer chain and two in the core (Odani, Shimma et al. 1996). One must note that as it stands nowadays, the acceptor of Ktr6p *in vivo* is unknown. Data suggests that, *in vitro*, the presence of an α-1,2-mannotriose is the minimal requirement for the enzyme to exhibit activity (Fig. 9) (Karson and Ballou 1978).

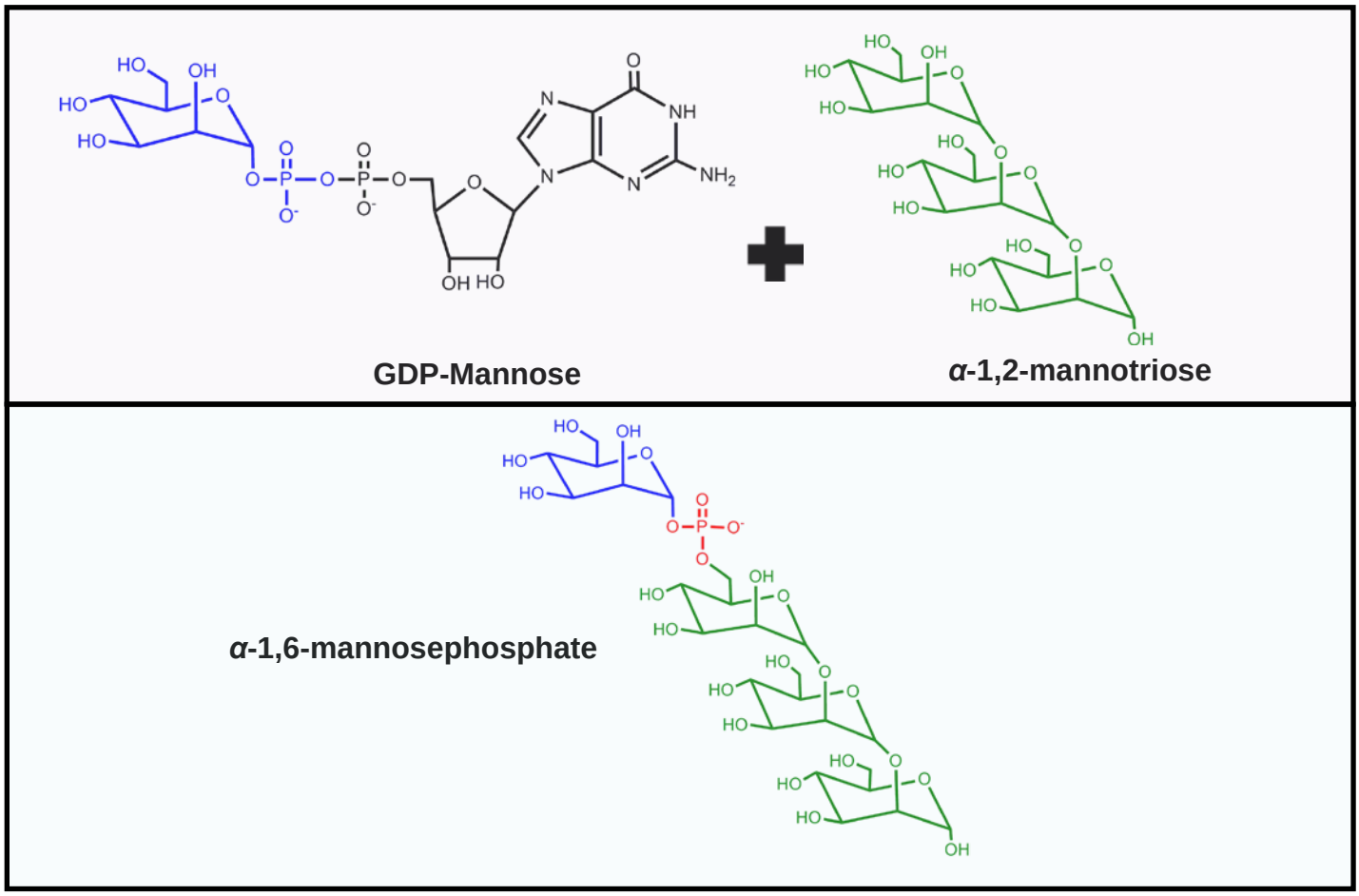

Figure 9: The proposed reaction scheme as catalyzed by Ktr6p.
All mannosyltransferases require GDP-mannose as a sugar donor. It has been proposed that the minimal acceptor species for Ktr6p is an *α*-1,2-mannotriose (green) (Karson and Ballou 1978). Ktr6p transfers the mannose-1-phosphate entity (blue) of GDP-mannose onto *α*-1,2-mannotriose, to form an *α*-1,6-mannosephosphate linkage (red).

1.3.4.1. Regulation of Ktr6p

In the early 1970's, mutational and complementation studies linked the mannosylphosphate transfer activity phenotype, in yeast mannan, to the *MNN4* (*mann*osyltransferase) gene (Ballou, Kern et al. 1973). Further investigations of the like led to the hypothesis that the protein, Mnn4p, functions as a positive regulator of Ktr6p (Karson and Ballou 1978). Mnn4p is found to be dependent on the cell growth phase, the cAMP levels and the extracellular environment (Odani, Shimma et al. 1997). It is believed that both proteins are required to be present in order for the mannosylphosphate transferase reaction to occur (Odani, Shimma et al. 1997). Furthermore, it has been observed that multiple copies of the *MNN4* gene augment transfer, whereas the copy-level of *KTR6* is irrelevant (Odani, Shimma et al. 1997).

An experiment designed to determine the time at which the reaction occurs during the *S. cerevisiae* life cycle involves collecting cultures at various time points and subjecting them to Alcian blue staining. Surprisingly, the yeast cells only stained blue during the stationary phase of growth (Jigami and Odani 1999). This suggests that the oligosaccharides may very well be synthesized during the logarithmic phase, but the mannose-1-phosphate decoration only occurs later on (Odani, Shimma et al. 1997). Likewise, cAMP levels decline during the stationary phase, and when researchers mutated genes in the cAMP pathway (i.e. PDE2-phosphodiesterase-2) to prematurely decrease the intracellular levels of cAMP, mannosylphosphate transfer occurred earlier (Jigami and Odani 1999). Attestation of these results stems from the transcriptional level of *MNN4*, which is induced only after 16 hours (Odani, Shimma et al. 1997). In contrast, the level of *KTR6* mRNA is held relatively constant throughout growth, meaning that enhancement of Mnn4p encourages phosphate transfer (Odani, Shimma et al. 1997). This mode of regulation resembles that of genes containing stress response elements (STREs) (Odani, Shimma et al. 1997). Coincidentally or not, *MNN4* does contain the STRE consensus sequence CCCCT, positioned upstream of the start codon (Odani, Shimma et al. 1997).

Incidentally, it is also believed that there is a greater rate of mannosylphosphate transfer during times of osmotic stress: it has been shown that in high salt solutions (i.e. 0.5 M KCl), *MNN4* mRNA levels are increased (Odani, Shimma et al. 1997).

A putative negative regulator of mannosylphosphate transfer has been identified as Mnn1p, which is normally responsible for the addition of the terminal α-1,3-mannose to both the core and outer chain (Jigami and Odani 1999).

1.3.5. Extensive Processing in *Saccharomyces cerevisiae*

As alluded to in a multitude of instances above, in yeast, the N-glycoproteins are sent to the Golgi to be further processed, elongated and decorated. Here, the enzymes involved and their postulated locations will be outlined in detail (Fig. 10).

The cisternae of the Golgi apparatus can be further subdivided into the *cis*-, *medial*- and *trans*-Golgi sectors, each characterized by a variance in the enzymes that they hold (Munro 2001). Generally, glycoproteins will enter via the *cis*-face and mature along with the cisternae, only to be released from the *trans*-face.

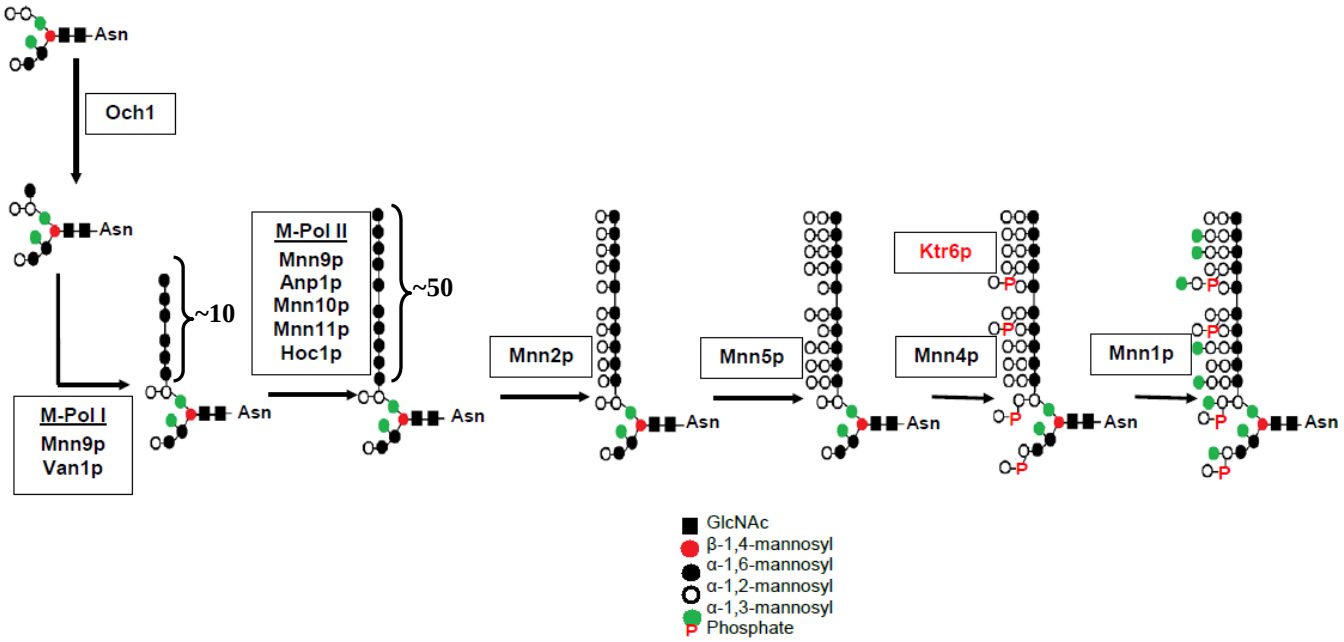

Figure 10: Elongation and decoration of glycoproteins in S. cerevisiae
As the glycoproteins progress through the maturing Golgi cisternae, they encounter different enzymes responsible for their modification, including Ktr6p, which is believed to add a mannose-1-phosphate to both the core and the outer branch.
Adapted from (Munro 2001)

Mannan biosynthesis is initialized at the *cis*-face when an α-1,6-mannose is attached to the core $Man_8GlcNAc_2$, as catalyzed by Och1p (*O*uter *Ch*ain elongation protein) (Munro 2001). From hereon, the glycoprotein is said to be primed for subsequent lengthening. The M-Pol I complex (*M*annan *Pol*ymerase), constituting of Mnn9p and Van1p (*Van*adate resistance protein), adds the first ten α-1,6-mannose residues (Munro 2001). It was found that a secondary complex, termed M-Pol II, serves to finalize the elongation by adding approximately forty mannose residues (Munro 2001). M-Pol II comprises five enzymes that fulfill its duties: Mnn9p, Mnn10p, Mnn11p, Anp1p (*A*mino*n*itrophenyl *p*ropanediol resistance protein) and Hoc1p (*H*omologous to *Oc*h1p) (Munro 2001). From this point onwards, α-1,2-mannose branching occurs first by Mnn2p, only to be followed by Mnn5p (Munro 2001). Kre2p, Ktr1p, Ktr3p may also partake in the addition of α-1,2-mannose to the outer chain. The reason for this functional redundancy remains unclear (Lussier, Sdicu et al. 1997). A select few branches can furthermore be decorated with α-1,6-mannosylphosphates through the action of Ktr6p (and, as mentioned above, a process which may be regulated by Mnn4p). Ultimately, Mnn1p caps off the branches with a terminal mannose via an α-1,3-linkage.

An appealing note to highlight is that the α-1,2- and α-1,3-mannose residues are predicted to be added in the *medial*-Golgi (Lussier 1999), and this particular spatial localization supports the idea that the presence of Mnn1p competes with Ktr6p activity.

The pathway presented above is not restricted to *Saccharomyces cerevisiae*, but can also be found in *Schizosaccharomyces pombe* and *Candida albicans* (Jigami and Odani 1999), 100-300 mannose sugars can be transferred to the core to form the elaborate outer chain (Munro 2001).

On the other hand, it is possible for the N-glycans that are initially sent to the Golgi to be simply modified on its core entity (e.g. vacuolar carboxypeptidase Y (Herscovics and Orlean 1993)). Och1p primes the molecule so that it may develop into $Man_{8\text{-}13}GlcNAc_2$. Ktr6p and Mnn1p also participate in this maturation process.

At long last, once the final product has reached the *trans*-face, the post-translationally modified protein is now able to enter the *trans*-Golgi network, destined to be secreted or to fulfill its role in cell wall maintenance.

The entire glycosylation pathway in yeast was put forth through means of many mutant constructs (Karson and Ballou 1978), and observing whether a change in glycan composition/phenotype could be detected. For example, Ktr6p was discovered through a comparison of *Δmnn1* with the *Δmnn1Δktr6* double mutant: the latter resulted in no Alcian blue staining (Wang, Nakayama et al. 1997). Similarly, for a triple mutant of *Δoch1Δmnn1Δktr6* (in this situation, outer chain elongation is inhibited), there is no Alcian blue staining as compared to *Δoch1Δmnn1* (Wang, Nakayama et al. 1997). These results strongly point in the direction that Ktr6p could very well be a mannosylphosphate transferase not only involved in outer chain glycosylation, but can also affect the core oligosaccharide.

1.3.6. Putative Role of Ktr6p/Mnn6p

Much of the research to date dictates that the purpose of adding mannosylphosphate to the glycoproteins may be to aid the cell in protecting itself from environmental factors. The net negative charge imparted by the phosphates (Karson and Ballou 1978) may lead to the formation of a hydration shell, and consequently, protect the cell surface proteins from situations where the salt concentrations fluctuate (Odani, Shimma et al. 1997). Defects in the mannosylphosphate transferase impinge upon cell wall integrity, but do not cause lethality (Jigami and Odani 1999).

1.4. Mannosephosphate in Pathogenic Fungal Species

Science is taking hold of the concept of the largely negative cell surface charge in terms of targeting yeast cells as a therapeutic means. *Candida albicans* is a normal member of the human microbiota, with a good standing relationship with its host (Hazen, Singleton et al. 2007). As of late, there has been a dramatic increase in numbers of fungal infections in immunocompromized individuals (Hobson, Munro et al. 2004). At this point, it is interesting to note that despite the fact that *C. albicans* lacks Ktr6p, its cell wall consists of many proteins that are

mannosylphosphorylated by Mnn4p (Hazen, Singleton et al. 2007). A new type of antifungal has been proposed, which takes advantage of the phosphorylated nature of these proteins.

Cationic peptides, produced in a wide variety of species (from bacteria to plants to amphibians), disrupt the cell wall (Harris, Mora-Montes et al. 2009). As mentioned above, mannosylphosphorylated proteins may not only be involved in interacting with the host or protecting against osmotic stress, they may also regulate porosity of the cell wall. As such, the cationic peptide will be able to dissipate and pass through this negatively-charged barrier to penetrate the cell (Harris, Mora-Montes et al. 2009).

Despite the results being premature, one such antifungal peptide is the α-helical compound, Dermaseptin, which relies on the presence of mannosephosphate being located on the cell wall in order to exert its effects. Mutants incapable of catalyzing this reaction are in fact resistant to the drug (Harris, Mora-Montes et al. 2009). Once the cell wall has been dismantled, the compound may insert itself into the plasma membrane, and lethality ensues.

1.5. Rationale of the Research

Studies on Ktr6p are sought out in order to confirm whether it shares significant structural homology with Kre2p, and if important motifs and/or residues can be identified. X-ray crystallography is an invaluable technique, providing researchers with a snapshot of the protein itself in a potentially catalytically active environment, and allowing one to ascertain the answers to the aforementioned questions. This information can be further supplemented with data obtained from Small-Angle X-ray Scattering (SAXS) to detect the behaviour of the protein in solution. In essence, our goal is to elucidate the three dimensional structure of Ktr6p.

CHAPTER II - MATERIALS AND METHODS

2.1. Materials

GDP-mannose was purchased from Sigma-Aldrich; Macro-Prep ceramic Hydroxyapatite Type I (20 μm) resin from Bio-Rad; Sephadex® G-15, Q-Sepharose™ resins, and Mono-Q™ 10/100 GL, and HiPrep™ 26/10 columns were from GE Healthcare Biosciences; protein crystallization suites were from Qiagen; 25% glutaraldehyde at pH 3 was obtained from Sigma-Aldrich; tetra methyl *ortho*-silicate was from Fluka; all chemicals were of reagent grade.

2.2. Initial Protein Purification and Crystallization Tests

The laboratory of Dr. Annette Herscovics from McGill University has graciously donated a *Pichia pastoris* protein construct of Ktr6p, spanning residues 99-446 (excluding the transmembrane domain and stem region), which was expressed as previously reported (Lobsanov, Romero et al. 2004). Macro-Prep ceramic hydroxyapatite and Q-Sepharose chromatography were employed to purify the medium. Protein fractions were pooled and dialyzed against 10 mM Tris-HCl pH 7.0, and concentrated to 60 mg/ml by centrifugal 10 kDa ultrafilters (Millipore).

2.2.1. Dynamic Light Scattering (DLS)

To characterize the protein's behavior in the selected storage buffer, 12 μl was pipetted into a quartz cuvette designed for DLS (DynaPro Molecular Sizing Instrument, Protein Solutions). Data acquisition (25ºC, 100% laser power, 10 second intervals) was accomplished with Dynamics V6 software; the polydispersity and radius of hydration were measured.

2.2.2. Crystallization Trials

Ktr6p was diluted to a concentration of 15 mg/ml prior to initiating crystallization trials (Table 1a). Equal volumes of protein and reservoir solutions, added to a final volume of 2 μl and with a reservoir volume of 100 μl, were mixed in Corning

96-well crystallography microplates by the MultiProbe II PLUS HT EX liquid handling robotic system (PerkinElmer), utilizing the sitting-drop vapour diffusion method. Plates were then incubated at 4ºC and 22ºC, and were inspected at three day intervals.

2.3. Development of a New Protein Purification Procedure

Expression of the Ktr6p construct was as formerly described (Lobsanov, Romero et al. 2004). The medium was filtered into 10 mM potassium phosphate (KH_2PO_4) pH 5.5. The filtrate was applied to a hydroxyapatite (HA) column (5x10 cm), equilibrated with 10 mM KH_2PO_4 pH 5.5, and the elution buffer, 0.5 M KH_2PO_4 pH 5.5. Protein fractions were pooled and desalted on a Sephadex G15 column (5x22 cm) equilibrated with 25 mM bis-tris propane pH 7.0. The eluted peaks were applied to a Q-Sepharose column (16x31 cm), equilibrated with buffer A (25 mM bis-tris propane pH 7.0) and buffer B (25 mM bis-tris propane pH 7.0, 1 M NaCl). The protein was eluted with a linear gradient (0-50% B) of buffer A to buffer B. The resulting fractions were once again desalted as described above and then applied to a Mono-Q 10/100 GL column. 2 ml of protein was injected onto the column at a time. A linear elution gradient was applied from buffer A (10 mM bis-tris propane pH 7.0) to buffer B (10 mM bis-tris propane pH 7.0, 0.5 M NaCl). The column was re-equilibrated with buffer A and another 2 ml of protein solution was injected. This process was repeated until the entire protein sample was consumed. Peaks A and B were isolated and separately desalted into 10 mM tris-HCl pH 7.0 on a HiPrep Desalting column. The fractions spanning the intermittent region between Peaks A and B were re-applied onto the Mono-Q, and then desalted. The final protein samples were concentrated to 15 mg/ml by centrifugal 10 kDa filter devices (Millipore). Protein fractions were identified from an SDS-PAGE.

a)

	Screen									
	$AmSO_4$	**Buffer**	**Classics**	**Classics II**	**JCSG I-IV**	**MPD**	**PACT**	**PEGs I**	**PEGs II**	**Opti-Salt**
Initial Purification	X		X	X	X	X	X	X	X	
New Purification (Peak A and B)		X			X		X	X	X	X

b)

	Screen				
	Additive	**Buffer**	**PEGs I**	**Opti-Salt**	**Glutaraldehyde**
0.1 M $CaCl_2$ and 10% PEG 3350					X
0.2 M Tri-Sodium Citrate and 20% PEG 3350	X	X		X	
TMOS			X		
5 mM Mn^{2+}			X		
5 mM GDP-mannose			X		
5 mM GDP-mannose, 5 mM Mn^{2+}			X		

Table 1: Suites involved in crystallization screens.
a) Sparse matrix screening prior to, and after, the development of the new purification procedure. b) Optimization of crystals and/or conditions obtained from brute force screening. The 0.1 M $CaCl_2$, 10% PEG 3350 crystals were cross-linked with glutaraldehyde. The 0.2 M Tri-sodium citrate, 20% PEG 3350 hit solution was combined with other screens. Chemical reagents, substrates and cofactors were also added to the protein solution in an attempt to optimize crystals.

2.4. The Newly Purified Ktr6p in Crystallization Trials

The new Ktr6p protein batch (15 mg/ml) was screened in a sitting-drop Qia2 plate (Qiagen) against different Qiagen Suites (Table 1a), at protein:well solution drop ratios of 0.5 μl:1.5 μl, 1 μl:1 μl, and 1.5 μl:0.5 μl, prepared by the Phoenix Liquid Handling System (Art Robbins Instruments). The reservoir volume was 100 μl. All plates were kept in a 22ºC incubator.

2.4.1. Crystal Optimization

The resulting crystals that grew in 0.2 M $CaCl_2$ and 20% PEG 3350 were optimized through the hanging-drop method in 24-well VDX plates (Hampton Research), and these were incubated at room temperature. The screen consisted of 70-120 mM $CaCl_2$ and 9-12% *(w/v)* PEG 3350.

Similarly, crystals grown in 0.2 M Tri-Sodium Citrate, 20% PEG 3350, were optimized against either a Buffer Screen or an Opti-Salt Screen (Table 1b).

2.4.2. Co-Crystallization of Ktr6p with its Donor

15 mg/ml of Ktr6p was incubated with 5 mM GDP-Mannose and/or its cofactor, 5 mM $MnCl_2$, for three hours on ice. Co-crystallization screens of Ktr6p in the presence of the substrate and cofactor were screened as described above in Qia2 sitting-drop plates by the MultiProbe II (Table 1b), but this time in MRC Triple-Drop plates with a reservoir volume of 45 μl (Molecular Dimensions).

2.5. Cross-linking Crystals with Glutaraldehyde

Crystals grown in 100 mM $CaCl_2$, 10% PEG 3350 were cross-linked by the gentle vapour diffusion method with 3 μl glutaraldehyde (Lusty 1999).

2.6. Tetra Methyl *Ortho*-Silicate (TMOS) and the *in gel* Crystallization Technique

A silica gel provided a support network for the growing of crystals (Moreno, Saridakis et al. 2002). The TMOS solution was prepared as directed (Moreno, Saridakis et al. 2002).

The TMOS stock solution was added to the PEGs I Suite to a final concentration of 0.2% (Table 1b). The three protein ratios as described above were tested for each condition in MRC Triple-Drop plates.

2.7. Small-Angle X-Ray Scattering (SAXS) *ab initio* Three Dimensional Reconstruction

Data collection of Ktr6p via SAXS was accomplished with the use of SAXSess mc^2 laboratory instrument from Anton Paar. Peak B protein samples, at concentrations of 15, 8, and 5 mg/ml, and storage buffer (10 mM Tris-HCl pH 7.0) scattering data were collected for 4 hour time periods at 4ºC. The two dimensional scattering pattern data acquisition and analysis was performed by utilizing SAXSquant 2.0 (Anton Paar).

Data collected at protein concentrations of 5 mg/ml was used for *ab initio* three dimensional shape reconstruction. Software, provided by ATSAS (GNOM (Svergun 1991), GASBOR (Svergun, Petoukhov et al. 2001), and DAMAVER (Volkov and Svergun 2003)), generated the most probable chain-compatible model of Ktr6p in solution.

2.8. Co-Crystallization Data Collection and Processing

Ktr6p crystals complexed with 5 mM GDP-Mannose grew in 0.1 M MES pH 6.5, 20% PEG 10,000. Three separate crystals were mounted inside MicroRT™ X-Ray Capillaries (MiTeGen), and three incomplete data sets were collected on a home-source rotating anode generator (MicroMax™-007 HF equipped with VariMax HF optics, Saturn944+ CCD (Rigaku Americas Corporation)) at room

temperature. The three data sets were subsequently processed and merged together with HKL2000 (Otwinowski and Minor 1997) to a final resolution of 3.11 Å.

2.9. Structure Solving and Refinement

The program Phaser was used to solve the phase problem by molecular replacement, using Kre2p (PDB Accession Code 1S4O) as the search model (McCoy, Grosse-Kunstleve et al. 2007). Alterations to the backbone, the input of Ktr6p-specific residues, and remodeling of loops 160-185 and 400-416 were performed manually using COOT (Emsley and Cowtan 2004). Alternating rounds of refinement with REFMAC5 (Murshudov, Vagin et al. 1997), CNS 1.2 (Brunger, Adams et al. 1998) and COOT led to the generation of a three dimensional model of Ktr6p. Calculation of the electrostatic surface involved the program APBS (Baker, Sept et al. 2001). The final refinement was done in REFMAC5. Superposition of the Ktr6p structure with the SAXS *ab initio* model was performed by SUPCOMB (Kozin and Svergun 2001). Figures were created with the use of PyMOL (DeLano).

CHAPTER III - RESULTS

3.1. Disparities between Purification Procedures

The original purification procedure resulted in the production of highly concentrated (60 mg/ml) Ktr6p, tinted with a hint of yellow. As viewed on an SDS-PAGE gel, the protein solution migrated to the appropriate molecular weight of 41 kDa, and showed little signs of impurities. Likewise, Dynamic Light Scattering data revealed that Ktr6p in a 10 mM Tris-HCl pH 7.0 buffer solution was stable, did not aggregate, and maintained a low polydispersity (Table 2). However, crystallization trials in over 2000 conditions immediately resulted in heavy precipitation, and there was no crystal growth.

Item	Time (s)	Temperature (ºC)	Radius of Hydration (nm)	Polydispersity (%)
Acq 1	9.3	21.8	2.2	14
Acq 2	19.3	23.5	2.3	18.1
Acq 3	29.3	24.4	2.3	23.5
Acq 4	39.3	24.7	2.2	22.5
Acq 5	49.4	24.8	2.3	17.4
Acq 6	59.4	24.9	2.2	16.4
Acq 7	69.4	24.9	2.2	10.8
Acq 8	79.4	24.9	2.2	14
Acq 9	89.4	24.9	2.2	22.8
Acq 10	99.4	24.9	2.2	16.4
Acq 11	109.4	25	2.2	30.6
Acq 12	119.4	25	2.2	24.8
Acq 13	129.5	25	2.2	19.3
Acq 14	139.5	25	2.2	10.1
Acq 15	149.5	25	2.1	22.8
Acq 16	159.5	25	2.1	26.2
Acq 17	169.6	25	2.2	33.2
Acq 18	179.6	25	2.1	18.5
Acq 19	189.6	25	2.2	23.2
Acq 20	199.6	25	2.1	25.5

Table 2: Dynamic Light Scattering data acquisition table.
The above table is one of many examples of data collected on Ktr6p. It was determined that 10 mM Tris-HCl pH 7.0 is a suitable buffer for our protein construct, as it favoured monomeric conformation of the protein, with a radius of hydration similar to that determined by SAXS.

In the new purification, running the filtrate on an HA column removed a significant amount of contaminants remaining from the media in which *P. pastoris* was grown, and Ktr6p is only found in Peak 2 (Fig. 12). Subsequent desalting into a 25 mM bis-tris propane pH 7.0 buffer allowed for the solution to be further cleansed through Q-Sepharose anion exchange chromatography. An additional anion exchange chromatographic step was added to verify that no other separation would occur, which was not the case. The Mono-Q 10/100 GL resolved the protein solution into two relatively distinct segments: Peak A and Peak B (Fig. 13). Finally, both peaks were isolated and desalted into 10 mM Tris-HCl pH 7.0, and concentrated to 15 mg/ml.

Peak A and B both contained Ktr6p, and both migrated to 41 kDa on an SDS-PAGE (Fig. 11). This was further confirmed by mass spectrometry, where little to no difference could be resolved between the two samples (data not shown).

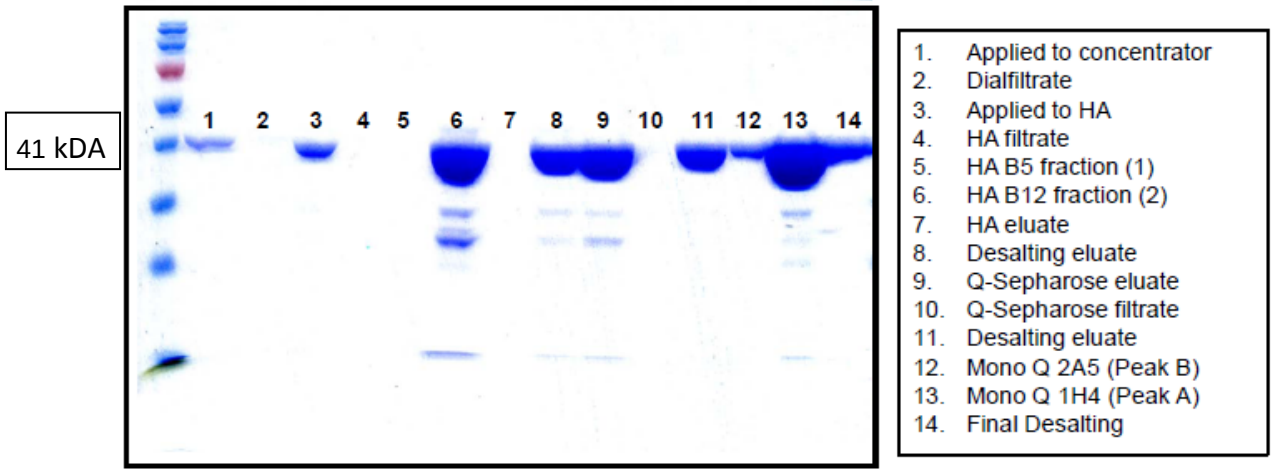

Figure 11: SDS-PAGE representing various stages of the new purification procedure.
Outlined above are various stages and column runs. Ktr6p migrated to 41kDa.

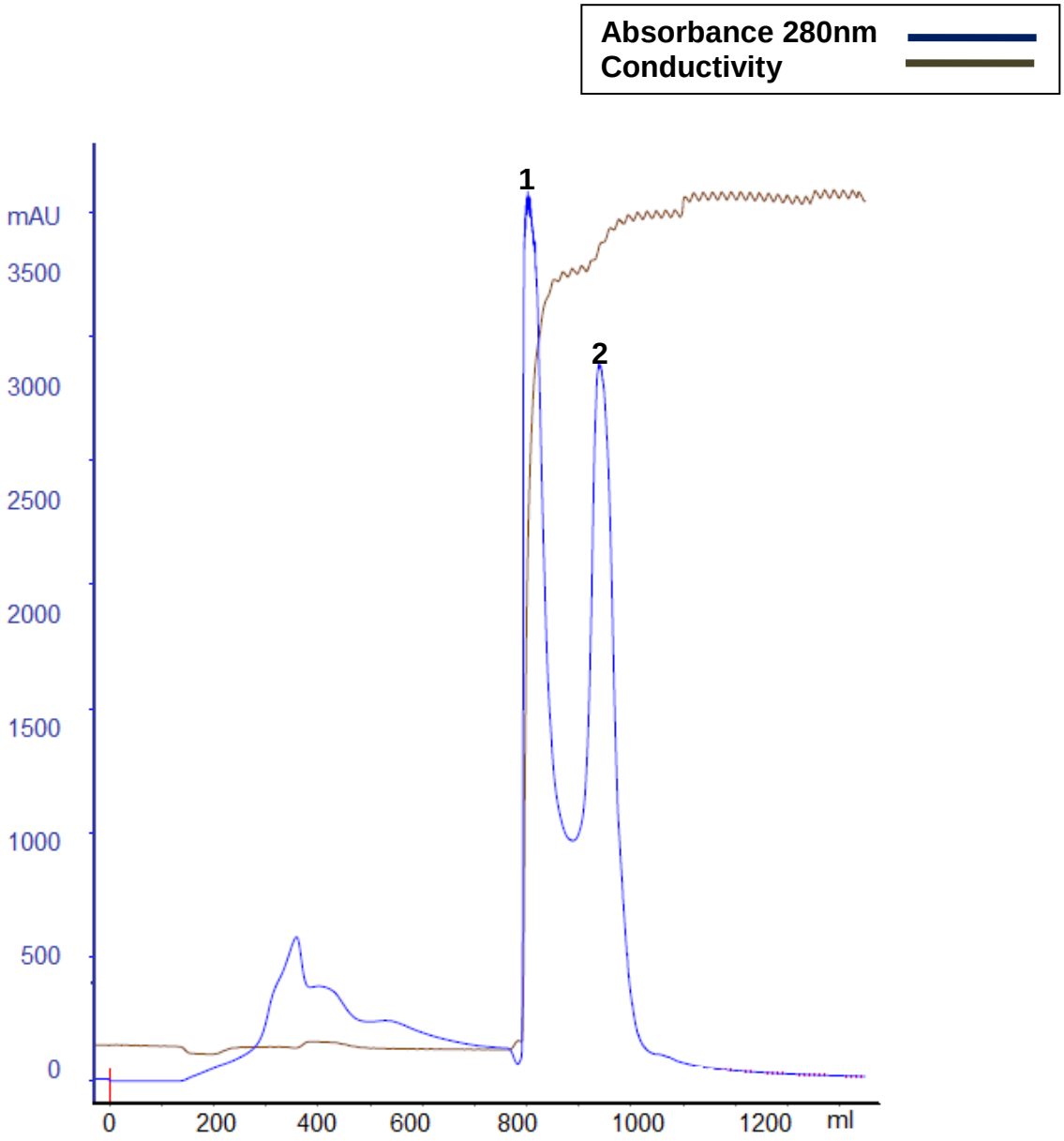

Figure 12: First purification step on an HA column.
The primary stage of the new purification procedure was able to efficiently remove residual contaminants from the yeast growth media. Consequently, the yellow tint that lingered during the original purification was no longer present. Ktr6p was only localized to Peak 2.

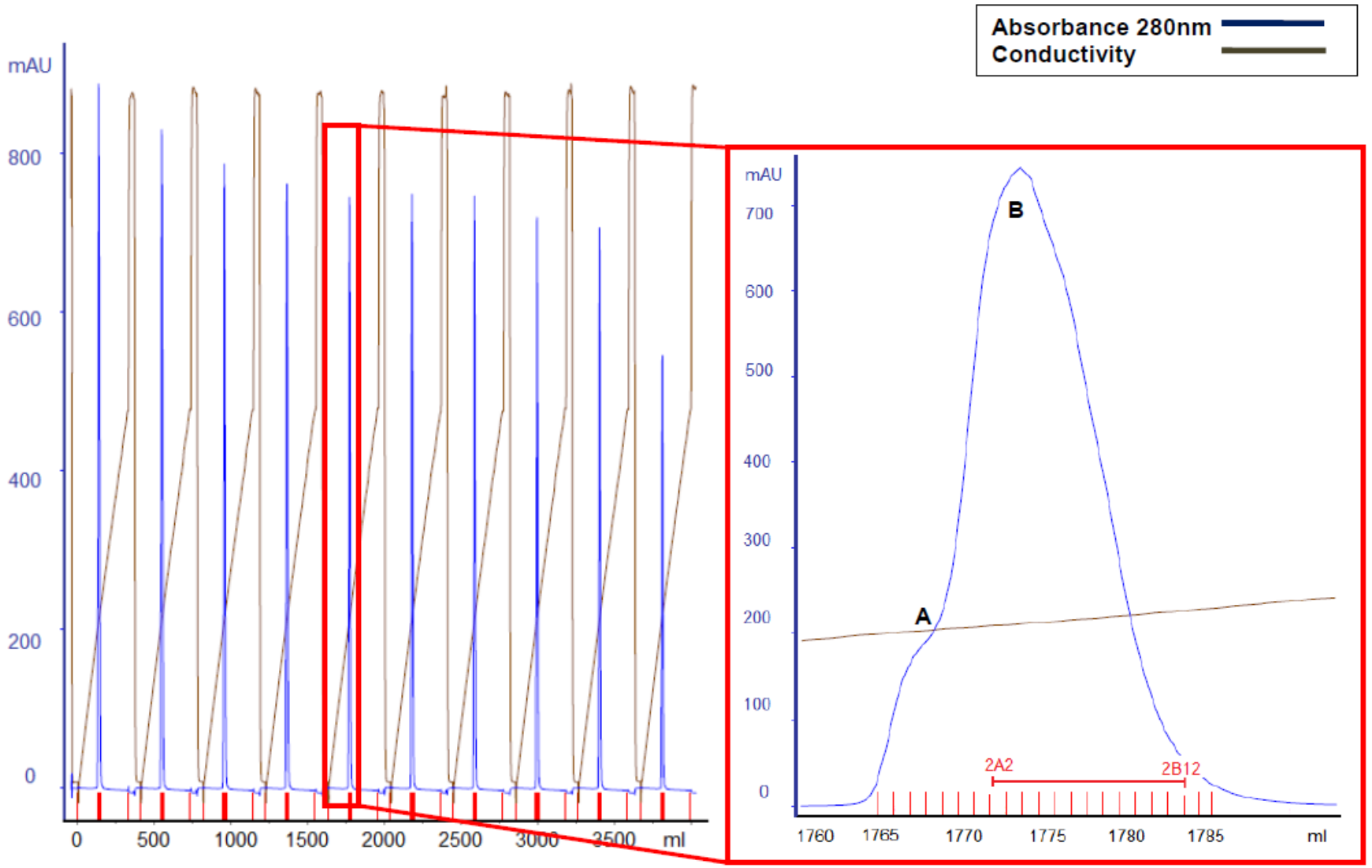

Figure 13: Automated Mono-Q GL 10/100.
Automatic injection of 2 ml protein solution (left) facilitated resolution of two peaks (right). Peak A impeded crystallization of Peak B (fractions 2A2-2B12).

3.2.Peak B Crystallization and Optimization

It is interesting to note that it was observed in crystallization trials that Peak A did not result in any crystal growth, and its presence impeded crystallization of Peak B. So, from this point onwards, it was not involved in any crystallization trials.

3.2.1. With Glutaraldehyde

Peak B formed microcrystals in a multitude of conditions, including 0.2 M $CaCl_2$, 20% PEG 3350 (Fig. 14a). Optimization in 24-well plates did little to improve nucleation, and of those screened for diffraction, no pattern could be resolved. Cross-linking the crystals grown in 100 mM $CaCl_2$, 10% PEG 3350 with glutaraldehyde for one hour did however generate a faint diffraction pattern.

3.2.2. With Buffer and Opti-Salt Screens

One month after the trays were set up, a new type of crystal was observed in 0.2 M Tri-Sodium Citrate, 20% PEG 3350, where a faint diffraction pattern was resolved to approximately 9 Å. Combining this hit solution with both a Buffer screen and an Opti-Salt screen produced significantly larger and better defined crystals (Fig. 14b and c). The resulting diffraction pattern did not indicate any improvement.

3.2.3. With Tetra Methyl *Ortho*-Silicate

Crystals grown in the presence of 0.2% TMOS were noticeable larger, where most wells contained only 2-3 crystals. This is a stark difference from the microcrystals that were normally cultivated. In particular, those grown in 0.1 M Tris-HCl pH 8.5 and 4.5M ammonium acetate, as well as 0.1 M sodium acetate pH 4.6 and 0.7 M $MgCl_2$, differentiated from the others in that they produced a diffraction pattern, albeit a weak one (Fig. 14d and e).

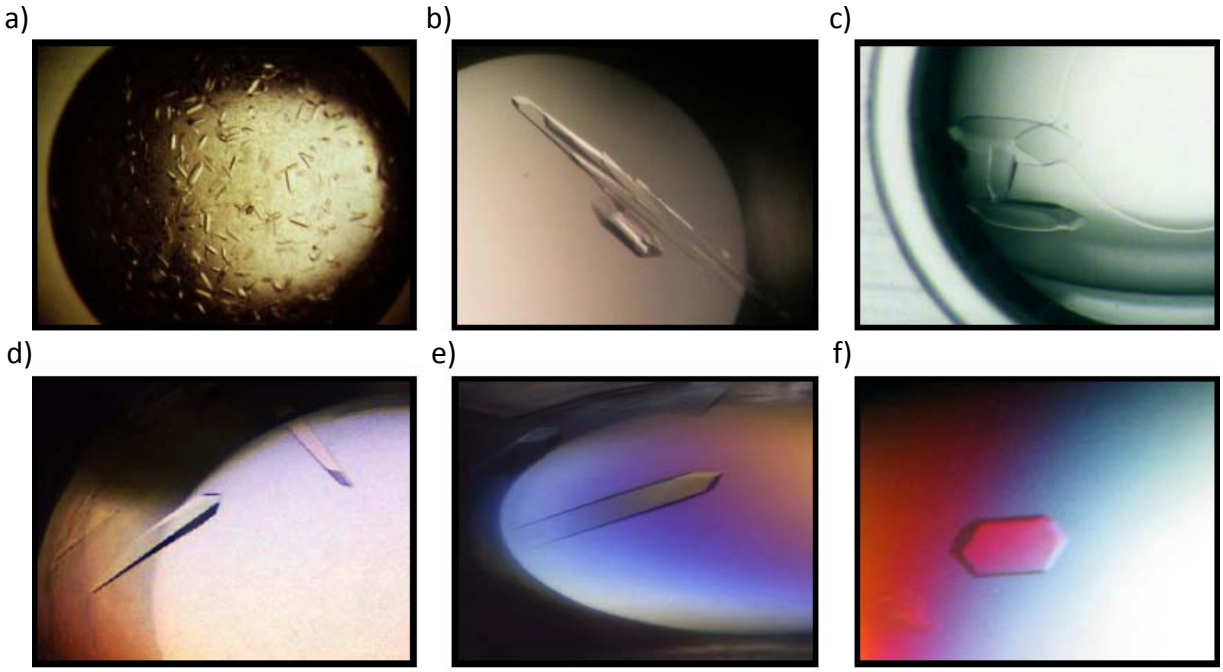

Figure 14: Crystals cultivated in different screens.
Cross-linking crystals in a) grown in 0.1M $CaCl_2$ and 10% PEG 3350 improved diffraction quality only slightly. The hit solution, 0.2M Tri-sodium citrate, was promising, but when combined with a Buffer Screen in b) or Opti-Salts in c), the resulting diffraction pattern was weak. Similar results were obtained when 0.2% TMOS was mixed with the well solutions from PEGs I Suite at different drop ratios: d) 1µl protein:1µl well of 0.1M sodium acetate pH 4.6 and 0.7M $MgCl_2$, e) 1.5µl protein:0.5µl well of 0.1 Tris-HCl pH 8.5 and 4.5M ammonium acetate. Finally, crystals grown in 0.1M MES pH 6.5 and 20% PEG 10,000 diffracted to 3.11 Å.

3.3. Ktr6p Co-Crystallization with GDP-Mannose and Structure Refinement

A new crystallization condition was discovered, after four weeks time, when Ktr6p was complexed to GDP-mannose: 0.1 M MES pH 6.5 and 20% PEG 10,000 (Fig. 14f). Not only was slow growth observed, but Ktr6p itself seemed particularly sensitive to the pH of the hit solution. So much so that crystals only grew in the stock solution provided by Qiagen. Furthermore, growth was also dependent on the type of plate used, and only occurred at 1 μl protein:1 μl well ratios in MRC Triple-Drop plates.

Crystals were harvested for screening at room temperature (Fig. 15). An incomplete data set was collected for three crystals, with each belonging to the $P2_12_12_1$ space group and containing 2 molecules per asymmetric unit. When merged, the final data set was resolved to 3.11 Å. A summary of the collection statistics can be found in Table 3.

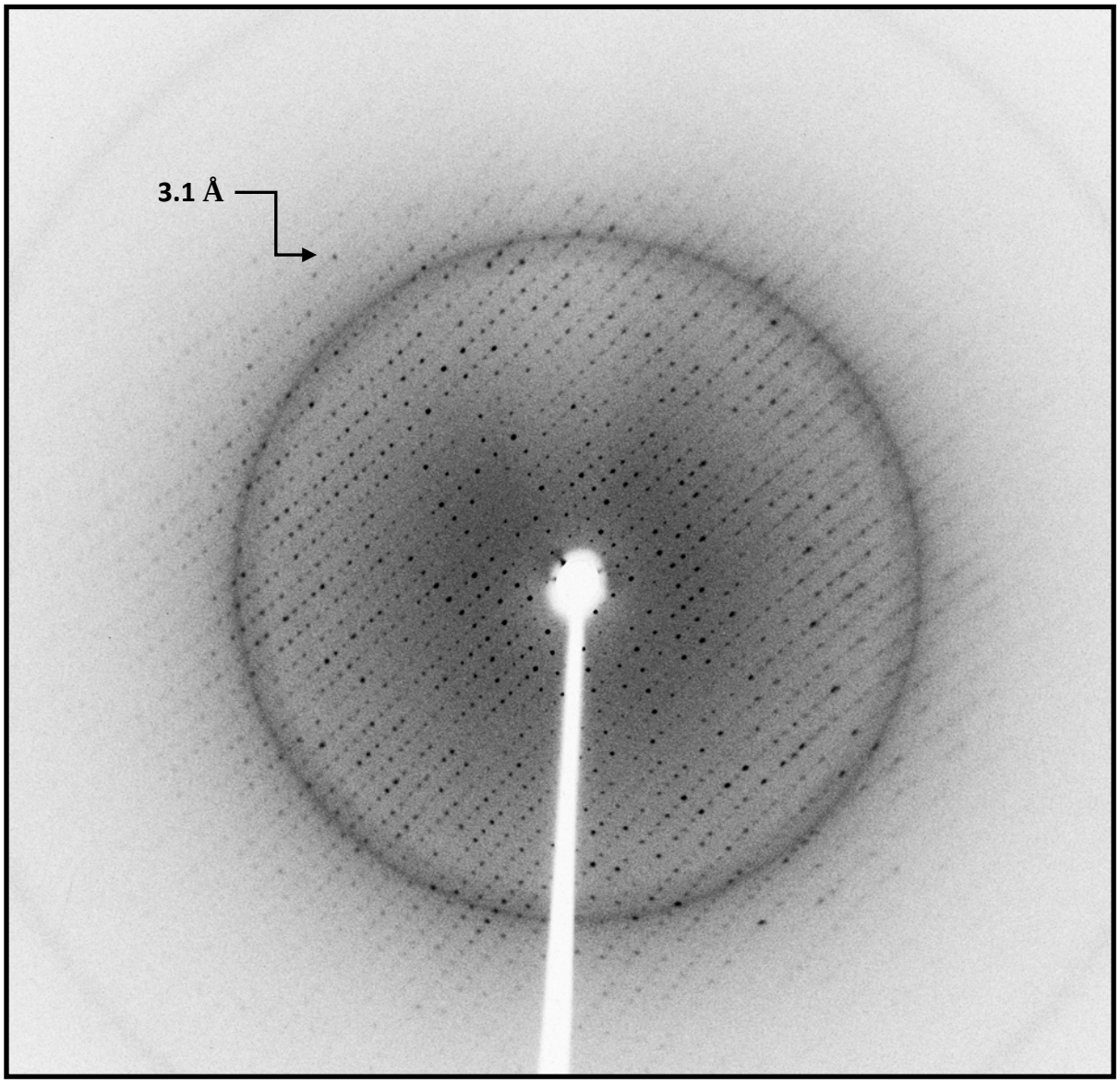

Figure 15: Diffraction Pattern obtained from a crystal grown in 0.1 M MES pH 6.5, 20% PEG 10000, 5 mM GDP-mannose.
The above image is a sample of those collected for three different crystals. Once indexed, merged and scaled together, the crystal structure of Ktr6p was resolved to 3.11 Å.

	Ktr6p
Resolution range (Å)	33.44-3.11 (3.15-3.10)
Space group	$P2_12_12_1$
a (Å)	65.164
b (Å)	107.401
c (Å)	113.255
α, β, γ (°)	90
Molecules per asymmetric unit	2
R_{merge}[a] (%)	13.1 (55.2)
R_{factor}[b] (%)	24.36
R_{free}[c] (%)	32.60
Number of unique reflections	14874 (718)
Redundancy	6.3 (6.1)
Completeness (%)	98.8 (99.6)
I/σ(I)	9.2
Root mean square deviation	
Bond length (Å)	0.028
Bond angles (°)	2.462
Ramachandran Plot[d] (%)	
Most favoured regions	76.7
Additional allowed regions	21.4
Generously allowed regions	1.6
Disallowed regions	0.3

[a] $R_{merge} = \Sigma|I - [I]| / \Sigma I$ where ***I*** is the measured intensity for symmetry-related reflections, and [*I*] is the mean intensity for the reflection.

[b] $R_{factor} = \Sigma (|Fo| - |Fc|) / \Sigma |Fo|$, where |Fo| is the observed and |Fc| is the calculated structure factor amplitude of a reflection.

[c] R_{free} was calculated by randomly omitting 10% of the observed reflections from the refinement.

[d] According to the Ramachandran plot in PROCHECK

Table 3: Data collection and refinement statistics for Ktr6p
Multiple crystals were scaled to obtain a complete data set.

Kre2p proved to be an efficient molecular replacement model. Phase refinement of the model resulted in a final figure-of-merit of 0.74. As a whole, Ktr6p fit well within the density, but residues 99-115 and 435-446 from Chains A and B had to be excluded due to lack of density. Much like its homolog, Ktr6 exemplified a single Type I Rossmann fold characteristic of GT-A family members in the N-terminal region of the molecule (Withers, Wakarchuk et al. 2002), with alternating α-helices and β-strands in the following topological array: $\downarrow\beta$1-(α-a)-$\downarrow\beta$2-(α-b)-$\downarrow\beta$3. Likewise, a mixed 7-stranded β-sheet lines the interior ($\downarrow\beta$3-$\downarrow\beta$2-$\downarrow\beta$1-$\downarrow\beta$4-$\uparrow\beta$9-$\downarrow\beta$6-$\downarrow\beta$10), and is flanked by an additional anti-parallel β-sheet ($\downarrow\beta$11-$\uparrow\beta$12-$\downarrow\beta$5) and C-terminal α-helices (Fig. 16). β11 and β12 are linked by a β-hairpin (residues 393-396). Furthermore, interspersed throughout the structure are five 3-10 helices. Finally, the three disulfide bonds that are conserved in most mannosyltransferases are positioned more towards the C-terminal region: C259-C411, C399-C413 and C327-C426.

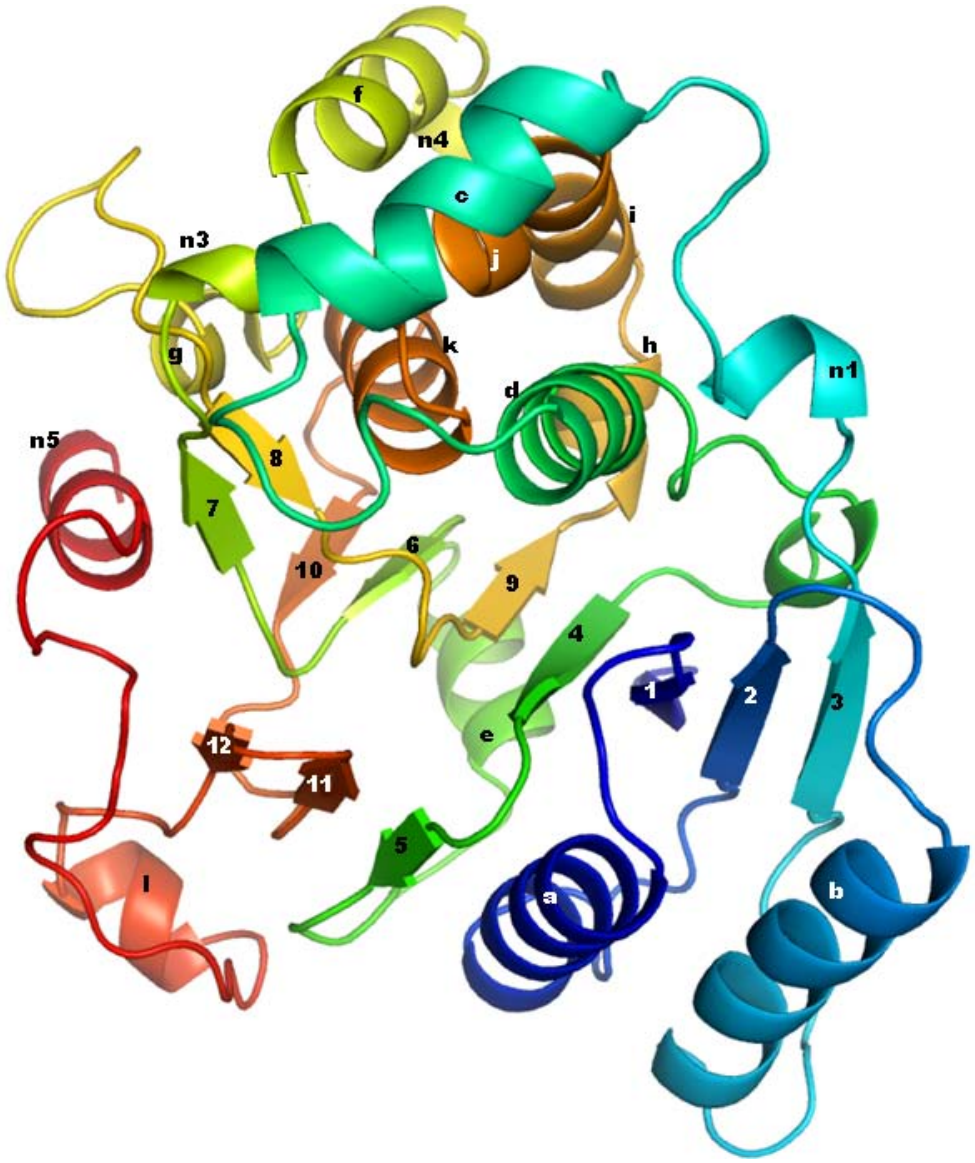

Figure 16: Atomic structure of Ktr6p.
Resolved to 3.11 Å, the crystal structure of Ktr6p exemplifies Type I Rossmann fold at its N-terminal region, as well as 7-stranded *β*-sheets sandwiched between anti-parallel *β*-sheets and *α*-helices. The progression of royal blue to red is representative of the movement from the N-terminus towards the C-terminus. Number codes reflect *β*-sheets; letters represent *α*-helices; and n, 3-10 helices. *β*1: 119-125, *α*-a: 131-145, *β*2: 152-157, *α*-b: 163-175, *β*3: 187-190, n1: 193-197, *α*-c: 204-214, *α*-d: 223-233, n2: 2240-243, *β*4: 247-250, *β*5: 255-257, *α*-e: 267-272, *β*6:276-278, *β*7: 281-283, n3: 286-288, *α*-f: 292-302, n4: 304-307, *α*-g: 313-316, *β*8: 327-329, *β*9: 335-337, *α*-h: 338-342, *α*-i: 344-356, *α*-j: 358-361, *α*-k: 366-376, *β*10: 383-385, *β*11: 396-398, *β*12: 391-393, *α*-l: 403-408, n5: 427-433.

As a whole, there was good agreement with the model constructed and the density with the exception of two flexible loop regions: residues 160-185 and 400-416. In contrast, those residues that span the putative active site (324-FNNCEFTSNFEI-335), as well as those located in the central 7-stranded β-sheet, fit well within the density. Additionally, the DXD motif, where in the case of Ktr6p it is 252-DPG-254, is also well defined (Fig. 17a and b). D394, from both Chains A and B are identified as the two Ramachandran plot outliers. This residue is located in the β-hairpin, which is positioned in the vicinity of the active site. Its role will be further elaborated on in the discussion.

Despite the incubation with GDP-mannose, density pertaining to the substrate could not be localized. It is possible that the GDP-mannose is simply a good additive to promote crystal formation, or that if the donor is positioned in the active site, it is disordered. Finally, if the enzyme is active and GDP-mannose is one of its substrates, then it is likely that Ktr6p cleaved the donor in the absence of the acceptor, as in the case of other glycosyltransferases (Lobsanov, Romero et al. 2004). If such a situation arose, then it is plausible that the enzyme would have a low affinity for the products, and these may have very well diffused away. Hence, the structure we present here is that of the apo-form.

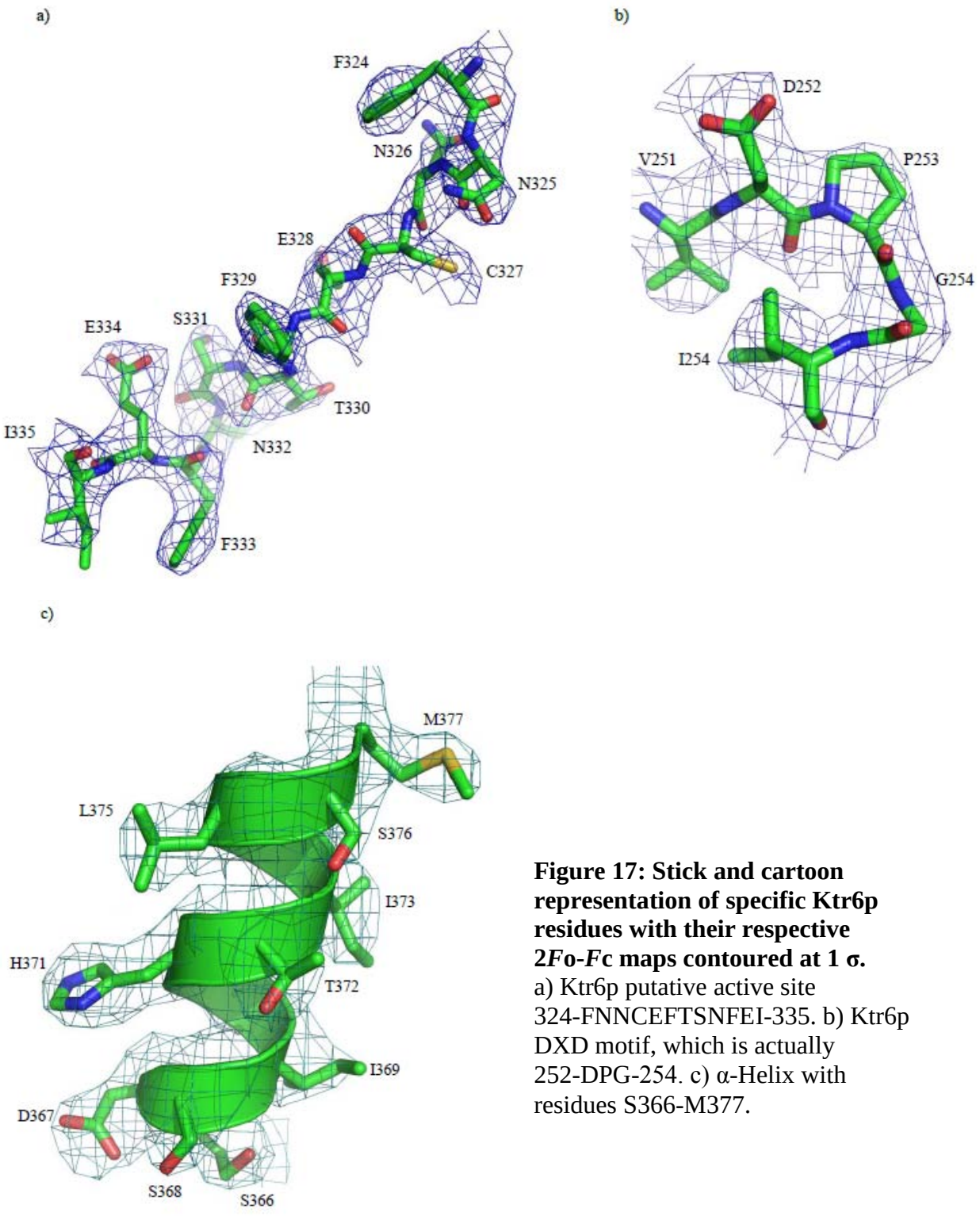

Figure 17: Stick and cartoon representation of specific Ktr6p residues with their respective 2*F*o-*F*c maps contoured at 1 σ. a) Ktr6p putative active site 324-FNNCEFTSNFEI-335. b) Ktr6p DXD motif, which is actually 252-DPG-254. c) α-Helix with residues S366-M377.

3.4. SAXS *ab initio* Model of Ktr6p in Solution

SAXS results revealed that no aggregation could be detected. Extrapolation of the radius of gyration (Rg) corresponded to that determined by DLS, 2.17 nm. Estimation of the molecular weight from the Rg also proved to be correct. Finally, the maximum dimension profile of Ktr6p in solution exemplified Gaussian distribution, indicative of a globular protein, spanning approximately 6 nm between its extremities.

Superposition of the *ab initio* model with the refined Ktr6p structure demonstrated high agreement, with a “distance after inertia axes alignment” of 0.4857, where values closer to 0 represent ideality (Fig. 18). This is indicative of the fact that the crystal structure that we have solved does not differ from that of Ktr6p in solution.

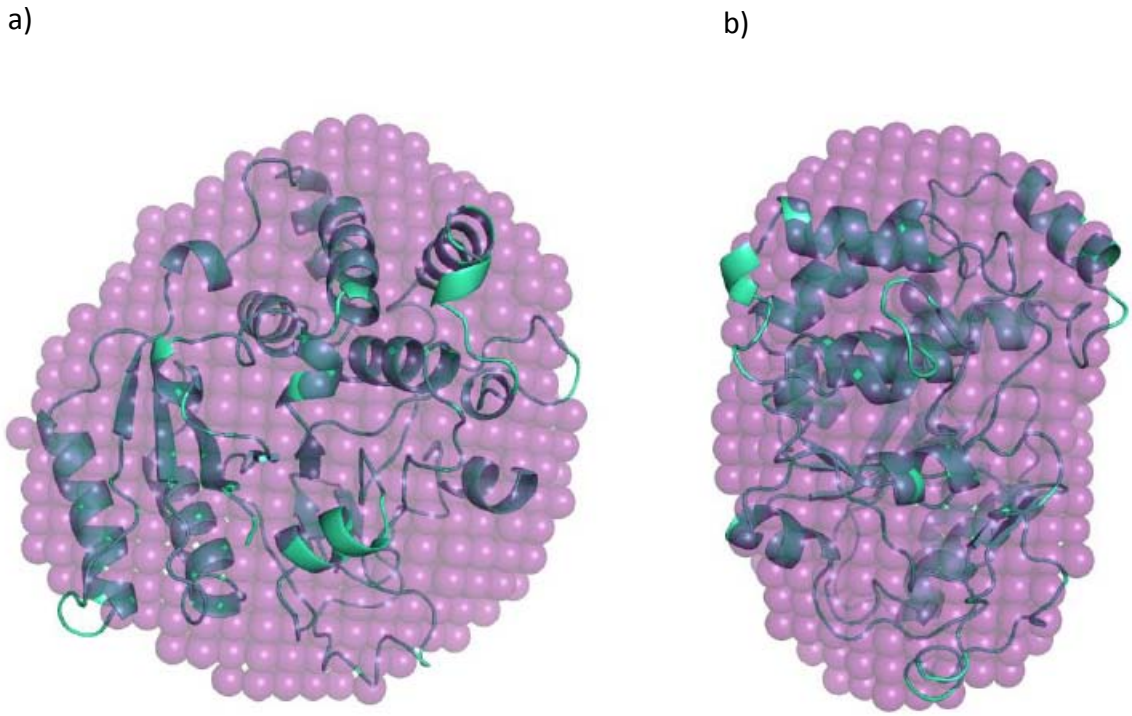

Figure 18: Relatedness of the Ktr6p crystal structure and the SAXS *ab initio* model.
Little differences may be observed between the atomic model (green) of Ktr6p and that of it in solution (purple). This is reflected by the "distance after inertia axes alignment", which is equal to 0.4857. a) Frontal view of the superimposed structure. b) Side view.

3.5. Summary of Results

Elaborate protein purification methods proved to be imperative in the progression of the project. The isolation of two distinct forms of Ktr6p allowed for the eventual crystal structure of the mannosylphosphate transferase to be resolved to 3.11 Å. Through the many crystal optimization screens, protein folding and organization were the primary obstacles to overcome. Only in the presence of its donor, GDP-mannose, could Ktr6p adopt a conformation that allowed for stable crystal growth and compactness. By means of X-Ray crystallography and SAXS, the behaviour of the atomic structure in both crystal and solution form could be observed, and they were found to be in high agreement with one another.

CHAPTER IV - DISCUSSION

4.1. The Ktr6p Structure in Relation to Other Transferases

Transferases specifically belonging to the GT-A family of glycosyltransferases are characterized by their single mixed α-β Rossmann fold. The mannosyltransferases involved in *S. cerevisiae* glycosylation are no exception, as was first shown in Kre2p, and now confirmed in a member of the same family, Ktr6p. Additionally, structural protein neighbours were identified by VAST, and not surprisingly, other glycosyltransferases of the GT-A family were retrieved, including: Kre2p (Rmsd 1.5), a putative mannose-1-phosphate guanylyltransferase (Rmsd 2.9) and glycogenin (Rmsd 3.2) (Madej, Gibrat et al. 1995).

4.2. A Detailed Comparison of Ktr6p and Kre2p

With the high degree of sequence similarity between Ktr6p and Kre2p, the use of an identical substrate donor, GDP-mannose, and the relatedness in their respective functions, it was anticipated that the homology between their three dimensional protein structures would be unequivocal (Fig. 19). The composition of the central β-sheet in Ktr6p parallels that in Kre2p, as does the flanking anti-parallel β-sheet. The juxtaposition of the surrounding α-helices in both structures on the other hand, does not conform identically in terms of position or length. This is also reflected in the flexibility of the adjoining loops, whose electron density in Ktr6p was at times deficient. It can be postulated that the absence of GDP-mannose in the Ktr6p structure accounts for this freedom of range, for in the Kre2p structure, where Mn^{2+} and GDP are present, these regions are stabilized.

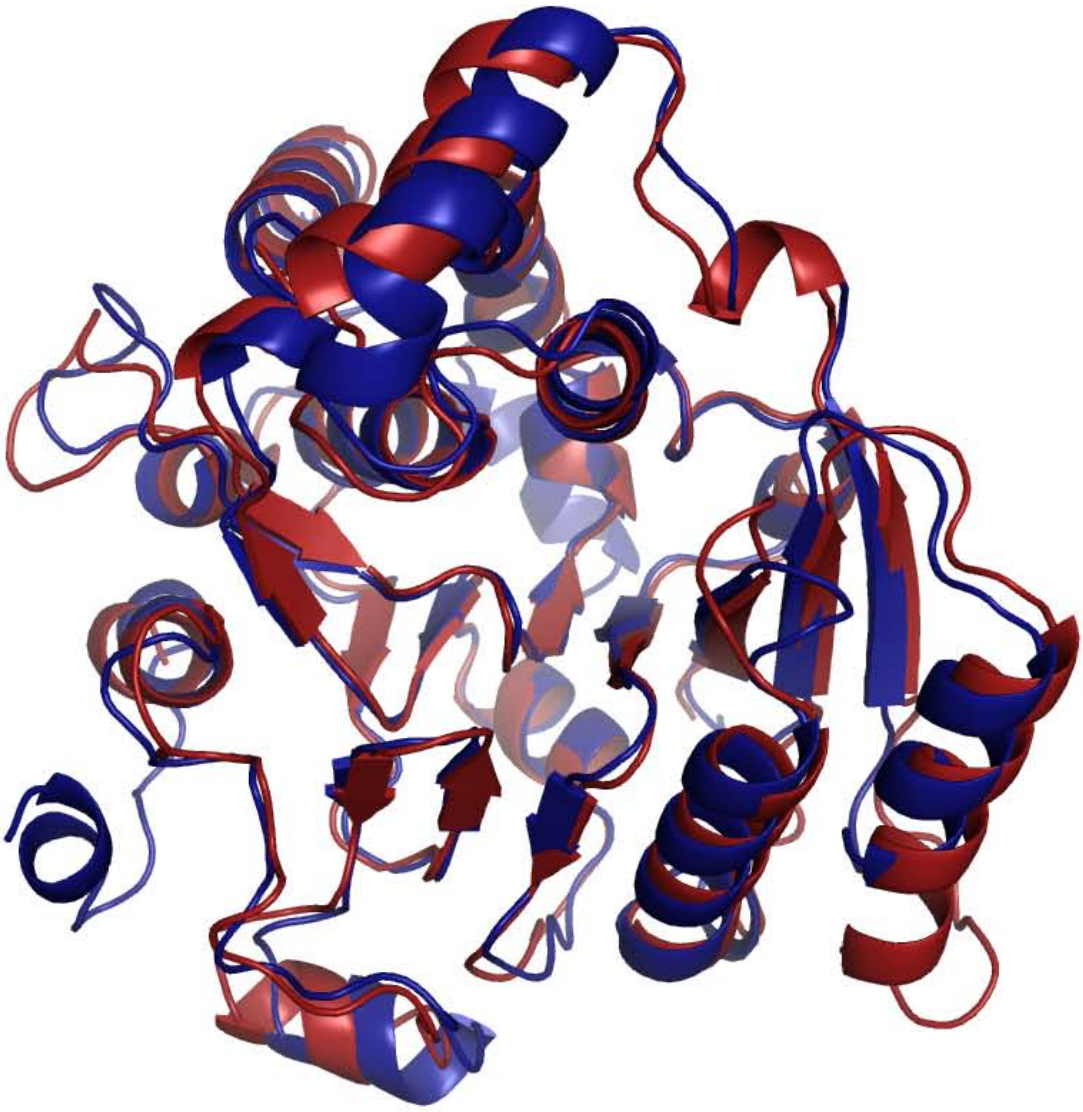

Figure 19: Superposition of Ktr6p and Kre2p.
Ktr6p (red) and Kre2p (blue) demonstrate a high degree of structural similarity, particularly amongst the 7-stranded β-sheet and the anti-parallel β-sheet. Divergence occurs in regions of higher flexibility, notably the flanking α-helices and loops. Other variances include the missing N-terminal and C-terminal helices in Ktr6, due to the lack of electron density.

The surface view of Ktr6p reveals that GDP-mannose, Mn^{2+}, and the acceptor species would position themselves within a cavity that lies along the central β-sheet (Fig. 20). This cavity is lined by 7-stranded β-sheet, β5, β7, β8, the β-hairpin, α-d, α-*k* and the loops between α-c/α-d and α-j/α-k, much like in Kre2p. In fact, this putative active site is fairly similar to that of Kre2p, as discussed below.

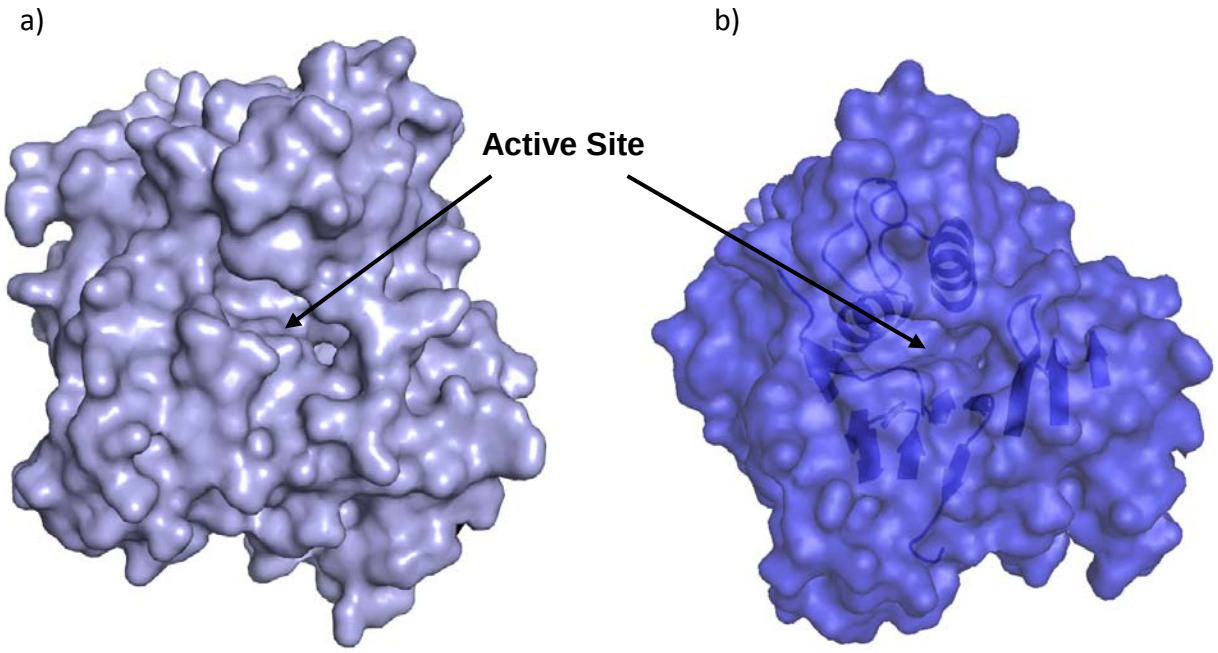

Figure 20: Surface view of Ktr6p.
a) Surface representation of Ktr6p, where the cavity positioned in the center of the molecule is defined as the putative active site. b) Surface and cartoon representation of the structural components that line the cavity.

4.2.1. A Look into the Putative Active site of Ktr6p

Based on sequence alignments, the following consensus sequence, FNNCEFTSNFEI, and the DXD variant, DPG, form the basis of the postulated active site in Ktr6p. The former slightly differs from the sequence found in Kre2p, YNLCHFWSNFEI, where primarily the substitution of tryptophan, in Kre2p, for threonine, in Ktr6p, can affect the local polarity and space in the cavity. On a similar note, the DXD variant of Ktr6p may have an analogous effect. Where in Ktr6p it is comprised of amino acids DPG, in Kre2p, it consists of EPD. From Figure 21, it can be visualized that the cavity belonging to Ktr6p is more negatively charged. Additionally, the area lining the DPG residues in Ktr6p appears to have a precise definition compared to the same location in Kre2p.

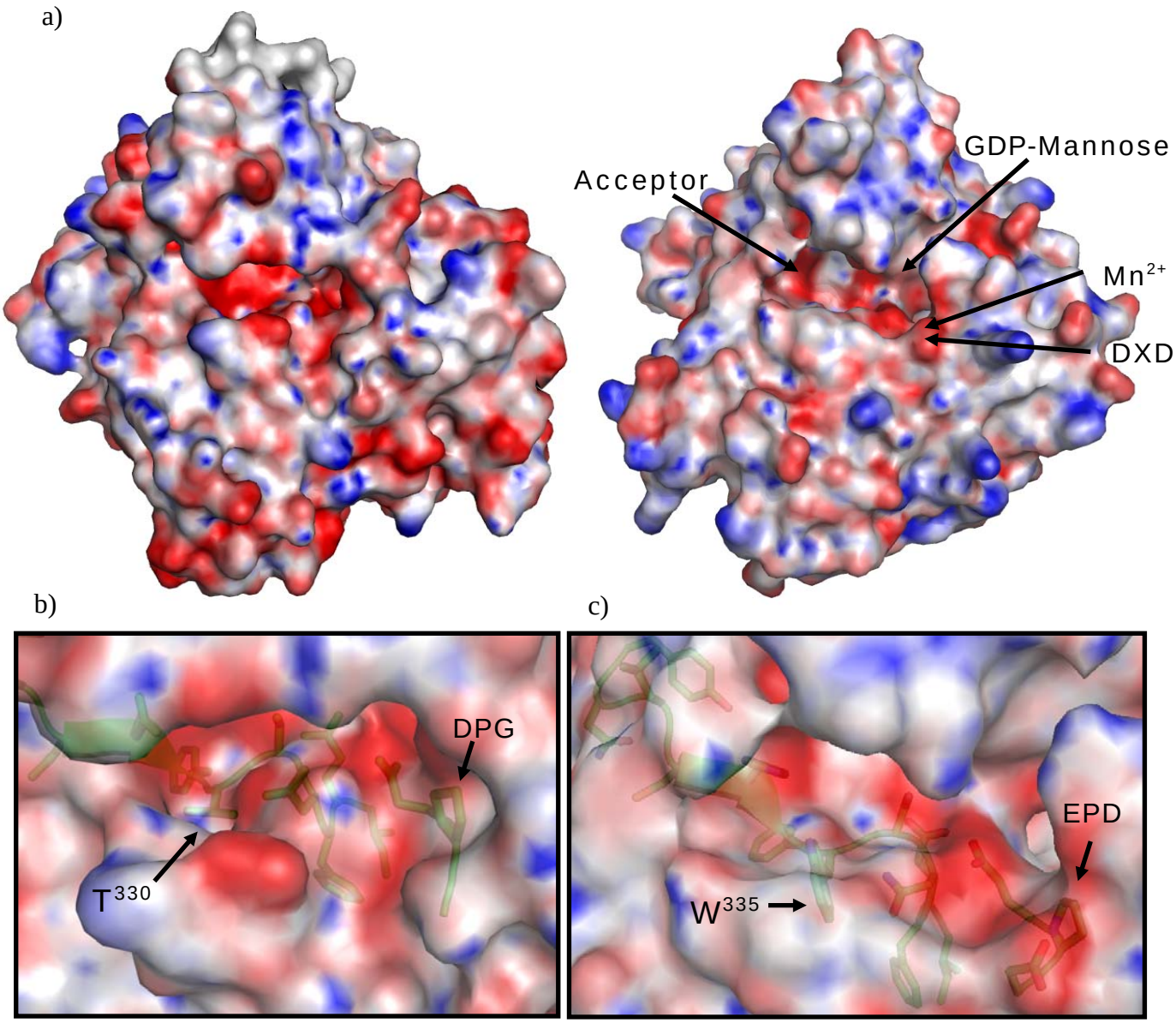

Figure 21: Electrostatics of Ktr6p and Kre2p
a) The electrostatic surface within the putative active site of Ktr6p (top left) is more negatively charged than that belonging to Kre2p (top right). The size of the postulated active site tends to appear larger in Ktr6p. The DXD region from Kre2p seems to cause the channel to protuberate. The proposed binding regions of manganese, the donor and acceptor species are also indicated on the Kre2p model. b) Stick model of the Ktr6 consensus sequence and DPG. The location of the Ktr6p threonine residue creates an indentation, whereas the tryptophan in Kre2p bulges outwards as shown in c. Red: negatively charged, blue: positively charged. Electrostatic maps computed by APBS (Baker, Sept et al. 2001).

Moreover, Lobsonov, Romero et al., have presented a reaction mechanism where they highlight specific residues that they suggest form important interactions with the donor, the substrate, the acceptor and the cofactor. Intriguingly, the majority of these amino acids are conserved throughout the KTR family, with the exception of Ktr6p, which may account for its role as a mannosylphosphate transferase. Below, a few key players are discussed in respect to the Ktr6p structure. Figure 22 outlines the residues postulated to interact with GDP-mannose and Mn^{2+}.

Lobsonov, Romero et al., suggest that the residues in the Kre2p β-hairpin, H^{387}-H^{388}-P^{389}-P^{390}-Y^{391} form a hydrophobic pocket that may act to stabilize the acceptor, and that H^{388} interacts with Mn^{2+} (Lobsanov, Romero et al. 2004). Also, they reveal that P^{390} is found in a *cis*-peptide conformation. Excuding Ktr6p, H^{388} is maintained throughout the KTR family. In fact, the β-hairpin residues of Ktr6p are the following: H^{392}-Y^{393}-D^{394}-Y^{395}-K^{396}, where Y^{393} distinctly protrudes outwards into the polarized active site (Fig. 23). Furthermore, H^{392} forms a hydrogen bond (2.83 Å) with D^{394}, thereby restricting its conformation. This constraint accounts for the Ramachandran plot outliers in both Chain A and Chain B.

The authors also believe that Y^{220} plays an important role in interacting with the Kre2p donor and acceptor species, for it is pointed down into the cavity. Once again, this tyrosine residue is conserved in eight of KTR members, all but in Ktr6p, where according to sequence alignments it is V^{225} (Fig 24a). Kinetic studies performed by the authors on a Y220F mutant do show a decrease in K_{cat} (Lobsanov, Romero et al. 2004). However, it has been determined in other glycosyltransferases that any residual activity remaining after such a presumably important mutation is indicative that the amino acid is not implicated in catalysis. If this were the case, based on similar experiments performed on retaining glucosidases, one would expect K_{cat} values of the mutant to be at least 10^{-5} fold of the wild type (Persson, Ly et al. 2001).

Keeping a similar theme in mind, the Kre2p residues coordinating the GDP phosphates, R^{130} and Y^{214}, are present in all family members, excluding Ktr6p. Here, the arginine is replaced by T^{126} and the tyrosine, by D^{219} (Fig 24b). This

dissimilarity could be one of the underlying factors as to why Ktr6p transfers mannose-1-phosphate as opposed to its family members, which are mannosyltransferases.

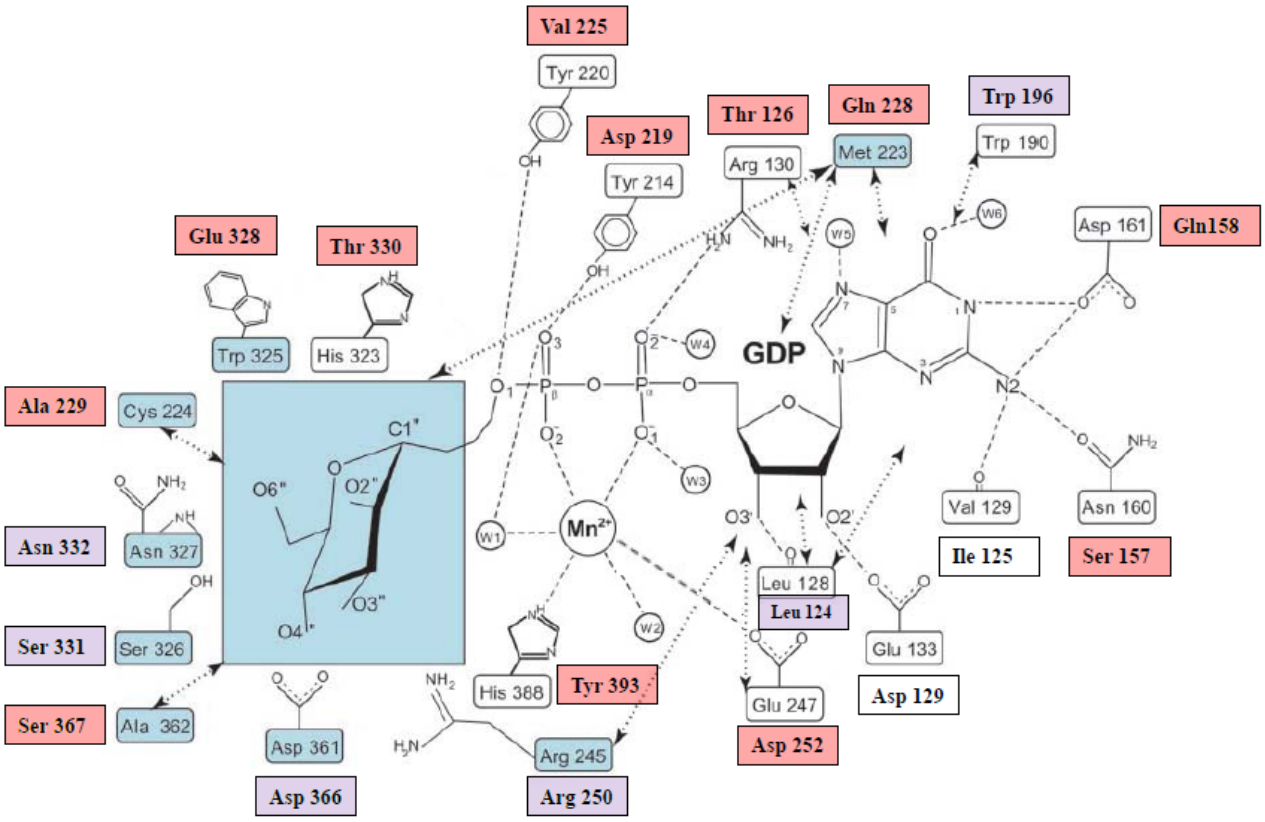

Figure 22: Amino acids in the active site interacting with GDP-mannose and Mn^{2+}

Schematic representation of the Kre2p amino acids that interact with the donor and cofactor. Those residues highlighted in blue are believed to interact with the sugar moiety. Corresponding Ktr6p amino acids are included and are shaded as follows: red (these residues are conserved in all KTR members except Ktr6p); purple (amino acids are found in all family members); white (no particular conservation scheme). Dashed lines indicate hydrogen bonds, dashed double-sided arrows are non-polar van der Waals interactions, circles represent water molecules.

Adapted from (Lobsanov, Romero et al. 2004)

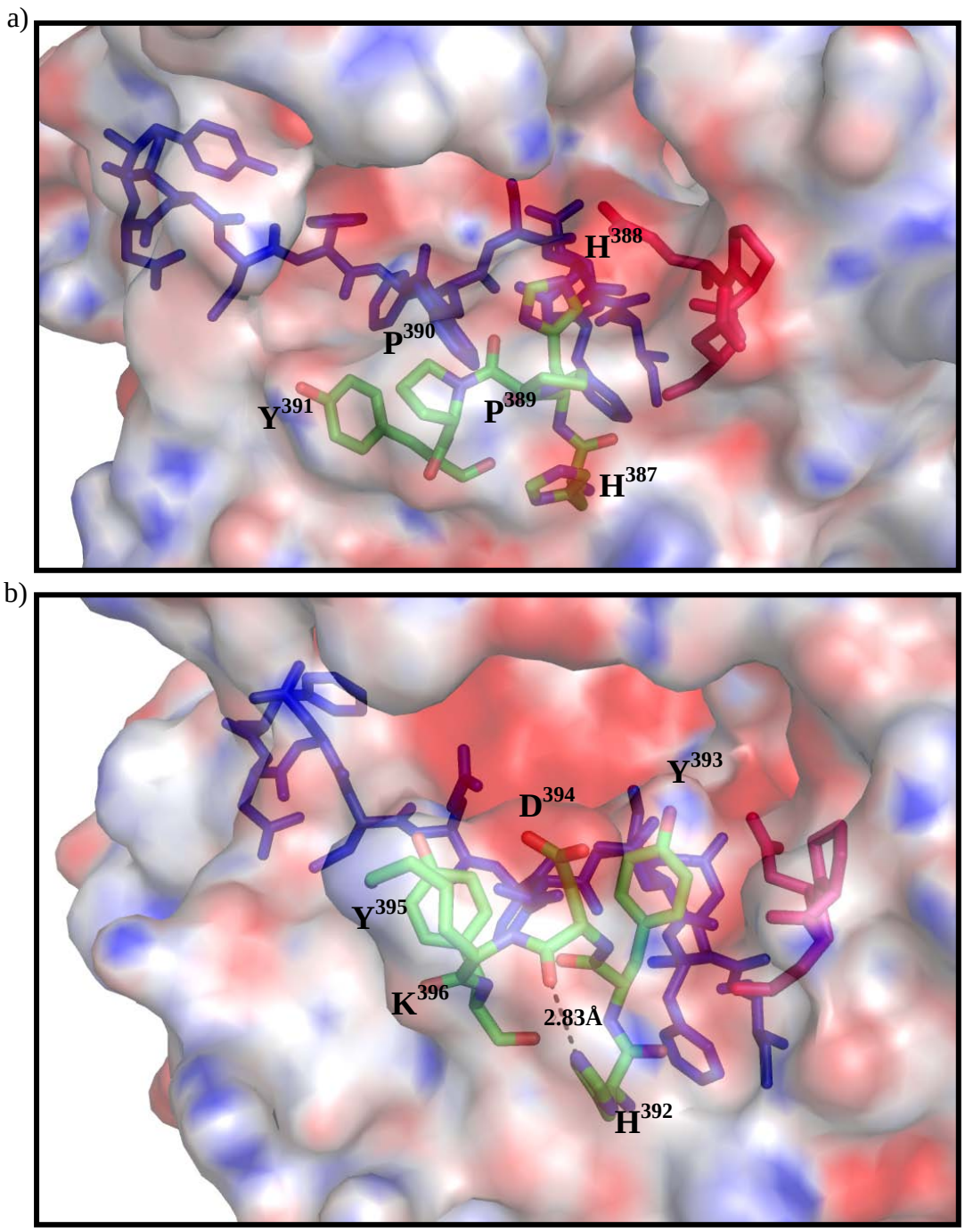

Figure 23: Representation of the *β*-hairpin in the Kre2p and Ktr6p active site.

a) The sequence, H-^{387}-H^{388}-P^{389}-P^{390}-Y^{391}, in Kre2p creates a relatively hydrophobic area presumably believed to facilitate interactions with manganese and the acceptor species. b) In Ktr6p, the H^{388} is not conserved, and is replaced by Y^{393}, which disrupts the surface of the active site. Additionally, the aspartic acid residue polarizes the region and due to the hydrogen bonding with H^{392}, it retains an unfavourable conformation according to Ramachandran statistics. The active site consensus sequence for both Kre2p and Ktr6p is shown in blue; the DXD variant, in pink.

a)

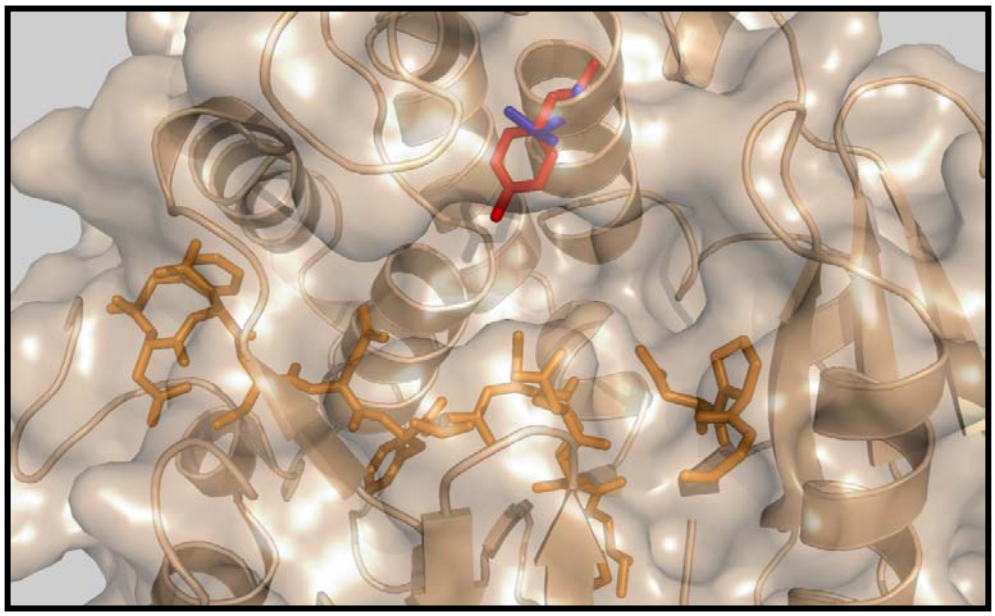

b)

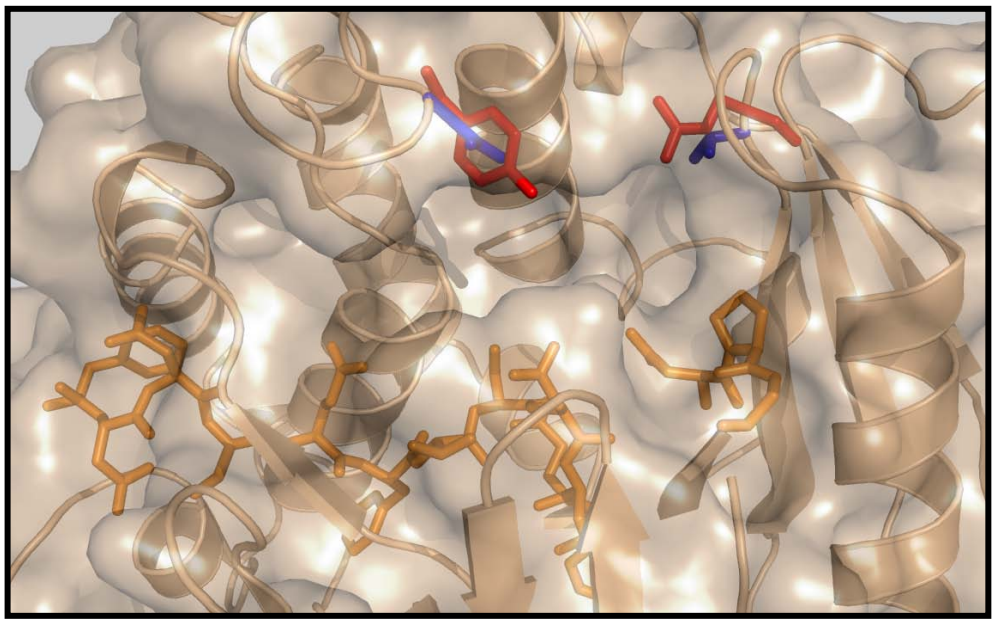

Figure 24: Localization of the Y^{220}, Y^{214} and R^{130} from Kre2p in respect to the Ktr6p active site

Cartoon representation of Ktr6p with the FNNCEFTSNFEI consensus sequence shown in orange. Stick representation of Kre2p is shown in red, and Ktr6p, in blue. a) Kre2p Y^{220} would extend far down into the active site to interact with GDP-mannose. Mutation of this amino acid does not inactivate the protein. Only in Ktr6p, is this residue replaced by V^{225}. b) Y^{214} and R^{130} in Kre2p coordinate the phosphates of GDP. In Ktr6p, the amino acids at these positions are D^{219} and T^{126} respectively.

The aforementioned findings may indeed reflect the necessary requirements that account for the differences existing between Ktr6p, Kre2p and the other members of the KTR family, in terms of the acceptor species and the catalytic mechanism. The conservation between key residues in 8/9 family members is astonishingly great, that the deviations in Ktr6p could potentially reflect its specific function. In Kre2p, it has been confirmed, *in vitro*, that methyl-α-mannoside, for example, behaves as the acceptor for the α-1,2-mannosyltransferase reaction (Lobsanov, Romero et al. 2004). In Ktr6p, an enzyme that allegedly creates an α-1,6-mannosephosphate bond, the *in vivo* acceptor remains undefined. It can be assumed that a slightly altered environment may be needed in order to transfer a mannose-1-phosphate from GDP-mannose, rather than simply a mannose residue.

CHAPTER V – CONCLUSIONS

The post-translational addition of sugar residues is a process that has been conserved throughout evolution. Its function is essential, its purpose is elusive. Despite the striking similarities, important differences do indeed exist between the process in higher eukaryotes and fungal species, particularly in the realm of core oligosaccharide elongation and decoration. In *Saccharomyces cerevisiae,* mannose-1-phosphate is one such decorative factor; its addition is catalyzed by the putative mannosylphosphate transferase Ktr6p. Putative for the reason that the *in vivo* acceptor has yet to be identified, for the reaction may be dependent on the presence of an Mnn4p/Ktr6p complex.

Through persistent purifications and crystal optimization, the structure of Ktr6p has been solved to a resolution of 3.11 Å. Not surprisingly, the degree of structural similarity between this enzyme and Kre2p, its homolog, is appreciatively strong. Slight diversity does exist within the active site, with that of Ktr6p appearing to be larger and more polar, perhaps accounting for the minor differences in their respective reactions.

Despite what may be, it has been shown through countless studies that the appearance of glycoproteins present on the cell wall that contain mannosephosphate, may play a valuable role in cell protection. Though *S. cerevisiae* itself may not be a threat, information extrapolated from its glycosylation pathway; the players involved and the effects each reaction step has on the cell (i.e. presence of mannosylphosphate on the cell wall) could be applicable to other fungal species.

BIBLIOGRAPHY

Abu-Qarn, M., J. Eichler, et al. (2008). "Not just for Eukarya anymore: protein glycosylation in Bacteria and Archaea." Curr Opin Struct Biol **18**(5): 544-550.

Alberts, B., A. Johnson, et al. (2002). Molecular Biology of the Cell. New York, Garland Science.

Apweiler, R., H. Hermjakob, et al. (1999). "On the frequency of protein glycosylation, as deduced from analysis of the SWISS-PROT database." Biochim Biophys Acta **1473**(1): 4-8.

Baker, N. A., D. Sept, et al. (2001). "Electrostatics of nanosystems: application to microtubules and the ribosome." Proc Natl Acad Sci U S A **98**(18): 10037-10041.

Ballou, C. E., K. A. Kern, et al. (1973). "Genetic control of yeast mannan structure. Complementation studies and properties of mannan mutants." J Biol Chem **248**(13): 4667-4671.

Bause, E. (1983). "Structural requirements of N-glycosylation of proteins. Studies with proline peptides as conformational probes." Biochem J **209**(2): 331-336.

Brunger, A. T., P. D. Adams, et al. (1998). "Crystallography & NMR system: A new software suite for macromolecular structure determination." Acta Crystallogr D Biol Crystallogr **54**(Pt 5): 905-921.

Burda, P. and M. Aebi (1998). "The ALG10 locus of Saccharomyces cerevisiae encodes the alpha-1,2 glucosyltransferase of the endoplasmic reticulum: the terminal glucose of the lipid-linked oligosaccharide is required for efficient N-linked glycosylation." Glycobiology **8**(5): 455-462.

Chaffin, W. L. (2008). "Candida albicans cell wall proteins." Microbiol Mol Biol Rev **72**(3): 495-544.

DeLano, W. L. "PyMOL Molecular Graphics System." from http://www.pymol.org.

Delgado, M. L., M. L. Gil, et al. (2003). "Candida albicans TDH3 gene promotes secretion of internal invertase when expressed in Saccharomyces cerevisiae as a glyceraldehyde-3-phosphate dehydrogenase-invertase fusion protein." Yeast **20**(8): 713-722.

Denisov, A. Y., P. Maattanen, et al. (2009). "Solution structure of the bb' domains of human protein disulfide isomerase." FEBS J **276**(5): 1440-1449.

Emsley, P. and K. Cowtan (2004). "Coot: model-building tools for molecular graphics." Acta Crystallogr D Biol Crystallogr **60**(Pt 12 Pt 1): 2126-2132.

Gentzsch, M. and W. Tanner (1996). "The PMT gene family: protein O-glycosylation in Saccharomyces cerevisiae is vital." EMBO J **15**(21): 5752-5759.

Gentzsch, M. and W. Tanner (1997). "Protein-O-glycosylation in yeast: protein-specific mannosyltransferases." Glycobiology **7**(4): 481-486.

Goon, S., C. P. Ewing, et al. (2006). "A sigma28-regulated nonflagella gene contributes to virulence of Campylobacter jejuni 81-176." Infect Immun **74**(1): 769-772.

Goto, M. (2007). "Protein O-glycosylation in fungi: diverse structures and multiple functions." Biosci Biotechnol Biochem **71**(6): 1415-1427.

Harris, M., H. M. Mora-Montes, et al. (2009). "Loss of mannosylphosphate from Candida albicans cell wall proteins results in enhanced resistance to the inhibitory effect of a cationic antimicrobial peptide via reduced peptide binding to the cell surface." Microbiology **155**(Pt 4): 1058-1070.

Hazen, K. C., D. R. Singleton, et al. (2007). "Influence of outer region mannosylphosphorylation on N-glycan formation by Candida albicans: normal acid-stable N-glycan formation requires acid-labile mannosylphosphate addition." Glycobiology **17**(10): 1052-1060.

Helenius, A. and M. Aebi (2004). "Roles of N-linked glycans in the endoplasmic reticulum." Annu Rev Biochem **73**: 1019-1049Odani, T., Y. Shimma, et al.

Helenius, J., D. T. Ng, et al. (2002). "Translocation of lipid-linked oligosaccharides across the ER membrane requires Rft1 protein." Nature **415**(6870): 447-450.

Herscovics, A. and P. Orlean (1993). "Glycoprotein biosynthesis in yeast." FASEB J **7**(6): 540-550.

Hill, K., C. Boone, et al. (1992). "Yeast KRE2 defines a new gene family encoding probable secretory proteins, and is required for the correct N-glycosylation of proteins." Genetics **130**(2): 273-283.

Hobson, R. P., C. A. Munro, et al. (2004). "Loss of cell wall mannosylphosphate in Candida albicans does not influence macrophage recognition." J Biol Chem **279**(38): 39628-39635.

Jentoft, N. (1990). "Why are proteins O-glycosylated?" Trends Biochem Sci **15**(8): 291-294.

Jigami, Y. (2008). "Yeast glycobiology and its application." Biosci Biotechnol Biochem **72**(3): 637-648.

Jigami, Y. and T. Odani (1999). "Mannosylphosphate transfer to yeast mannan." Biochim Biophys Acta **1426**(2): 335-345.

Karson, E. M. and C. E. Ballou (1978). "Biosynthesis of yeast mannan. Properties of a mannosylphosphate transferase in Saccharomyces cerevisiae." J Biol Chem **253**(18): 6484-6492.

Kostova, Z. and D. H. Wolf (2003). "For whom the bell tolls: protein quality control of the endoplasmic reticulum and the ubiquitin-proteasome connection." EMBO J **22**(10): 2309-2317.

Kozin, M. B. and D. I. Svergun (2001). "Automated matching of high- and low-resolution structural models." Journal of Applied Crystallography **34**: 33-41.

Kukuruzinska, M. A., M. L. Bergh, et al. (1987). "Protein glycosylation in yeast." Annu Rev Biochem **56**: 915-944.

Lehle, L., S. Strahl, et al. (2006). "Protein glycosylation, conserved from yeast to man: a model organism helps elucidate congenital human diseases." Angew Chem Int Ed Engl **45**(41): 6802-6818.

Lesage, G. and H. Bussey (2006). "Cell wall assembly in Saccharomyces cerevisiae." Microbiol Mol Biol Rev **70**(2): 317-343.

Lippincott-Schwartz, J., J. S. Bonifacino, et al. (1988). "Degradation from the endoplasmic reticulum: disposing of newly synthesized proteins." Cell **54**(2): 209-220.
Liu, M., A. Borgert, et al. (2008). "Conformational consequences of protein glycosylation: preparation of O-mannosyl serine and threonine building blocks, and their incorporation into glycopeptide sequences derived from alpha-dystroglycan." Biopolymers **90**(3): 358-368.

Lobsanov, Y. D., P. A. Romero, et al. (2004). "Structure of Kre2p/Mnt1p: a yeast alpha1,2-mannosyltransferase involved in mannoprotein biosynthesis." J Biol Chem **279**(17): 17921-17931.

Lussier, M., A. M. Sdicu, et al. (1999). "The KTR and MNN1 mannosyltransferase families of Saccharomyces cerevisiae." Biochim Biophys Acta 1426(2): **1426**(2): 323-334.

Lussier, M., A. M. Sdicu, et al. (1997). "The Ktr1p, Ktr3p, and Kre2p/Mnt1p mannosyltransferases participate in the elaboration of yeast O- and N-linked carbohydrate chains." J Biol Chem **272**(24): 15527-15531.

Lussier, M., A. M. Sdicu, et al. (1999). "The KTR and MNN1 mannosyltransferase families of Saccharomyces cerevisiae." Biochim Biophys Acta **1426**(2): 323-334.

Lusty, C. J. (1999). "A gentle vapor-diffusion technique for cross-linking of protein crystals for cryocrystallography." Journal of Applied Crystallography **32**: 106-112.

Maattanen, P., G. Kozlov, et al. (2006). "ERp57 and PDI: multifunctional protein disulfide isomerases with similar domain architectures but differing substrate-partner associations." Biochem Cell Biol **84**(6): 881-889.

Madej, T., J. F. Gibrat, et al. (1995). "Threading a database of protein cores." Proteins **23**(3): 356-369.

Marshall, R. D. (1974). "The nature and metabolism of the carbohydrate-peptide linkages of glycoproteins." Biochem Soc Symp(40): 17-26.

McCoy, A. J., R. W. Grosse-Kunstleve, et al. (2007). "Phaser crystallographic software." J Appl Crystallogr **40**(Pt 4): 658-674.

Mellquist, J. L., L. Kasturi, et al. (1998). "The amino acid following an asn-X-Ser/Thr sequon is an important determinant of N-linked core glycosylation efficiency." Biochemistry **37**(19): 6833-6837.

Messner, P. (2004). "Prokaryotic glycoproteins: unexplored but important." J Bacteriol **186**(9): 2517-2519.

Messner, P. (2009). "Prokaryotic protein glycosylation is rapidly expanding from "curiosity" to "ubiquity"." Chembiochem **10**(13): 2151-2154.

Moreno, A., E. Saridakis, et al. (2002). "Combination of oils and gels for enhancing the growth of protein crystals." Journal of Applied Crystallography **35**: 140-142.

Munro, S. (2001). "What can yeast tell us about N-linked glycosylation in the Golgi apparatus?" Febs Letters **498**(2-3): 223-227.

Murrell, M. P., K. J. Yarema, et al (2004). "The systems biology of glycosylation." Chembiochem **5**(10): 1334-1347.

Murshudov, G. N., A. A. Vagin, et al. (1997). "Refinement of macromolecular structures by the maximum-likelihood method." Acta Crystallogr D Biol Crystallogr **53**(Pt 3): 240-255.

Odani, T., Y. Shimma, et al. (1996). "Cloning and analysis of the MNN4 gene required for phosphorylation of N-linked oligosaccharides in Saccharomyces cerevisiae." Glycobiology **6**(8): 805-810.

Odani, T., Y. Shimma, et al. (1997). "Mannosylphosphate transfer to cell wall mannan is regulated by the transcriptional level of the MNN4 gene in Saccharomyces cerevisiae." FEBS Lett **420**(2-3): 186-190.

Otwinowski, Z. and W. Minor (1997). "Processing of X-ray diffraction data collected in oscillation mode." Macromolecular Crystallography, Pt A **276**: 307-326.

Parodi, A. J. (2000). "Protein glucosylation and its role in protein folding." Annu Rev Biochem **69**: 69-93.

Persson, K., H. D. Ly, et al. (2001). "Crystal structure of the retaining galactosyltransferase LgtC from Neisseria meningitidis in complex with donor and acceptor sugar analogs." Nat Struct Biol **8**(2): 166-175.

Romero, P. A., M. Lussier, et al. (1999). "Mnt2p and Mnt3p of Saccharomyces cerevisiae are members of the Mnn1p family of alpha-1,3-mannosyltransferases responsible for adding the terminal mannose residues of O-linked oligosaccharides." Glycobiology **9**(10): 1045-1051.

Schrader, E. K., K. G. Harstad, et al. (2009). "Targeting proteins for degradation." Nat Chem Biol **5**(11): 815-822.

Schwarz, M., R. Knauer, et al. (2005). "Yeast oligosaccharyltransferase consists of two functionally distinct sub-complexes, specified by either the Ost3p or Ost6p subunit." FEBS Lett **579**(29): 6564-6568.
Shental-Bechor, D. and Y. Levy (2008). "Effect of glycosylation on protein folding: a close look at thermodynamic stabilization." Proc Natl Acad Sci U S A **105**(24): 8256-8261.

Shental-Bechor, D. and Y. Levy (2009). "Folding of glycoproteins: toward understanding the biophysics of the glycosylation code." Curr Opin Struct Biol **19**(5): 524-533.

Sigma-Aldrich. "Yeast Cell Wall." from http://www.sigmaaldrich.com/life-science/metabolomics/enzyme-explorer/learning-center/lysing-enzymes.html.

Spiro, R. G. (2000). "Glucose residues as key determinants in the biosynthesis and quality control of glycoproteins with N-linked oligosaccharides." J Biol Chem **275**(46): 35657-35660.

Spiro, R. G. (2002). "Protein glycosylation: nature, distribution, enzymatic formation, and disease implications of glycopeptide bonds." Glycobiology **12**(4): 43R-56R.

Strahl-Bolsinger, S., M. Gentzsch, et al. (1999). "Protein O-mannosylation." Biochim Biophys Acta **1426**(2): 297-307.

Strahl-Bolsinger, S. and A. Scheinost (1999). "Transmembrane topology of Pmt1p, a member of an evolutionarily conserved family of protein O-mannosyltransferases." Journal of Biological Chemistry **274**(13): 9068-9075.

Svergun, D. I. (1991). "Mathematical-Methods in Small-Angle Scattering Data-Analysis." Journal of Applied Crystallography **24**: 485-492.

Svergun, D. I., M. V. Petoukhov, et al. (2001). "Determination of domain structure of proteins from X-ray solution scattering." Biophysical Journal **80**(6): 2946-2953.

Varki, A., R. Cummings, et al. (1999). Essentials of Glycobiology. Cold Spring Harbor, NY, Cold Spring Habor Laboratory Press.

Voet, D. and J. Voet (2004). Biochemistry. New York, J Wiley Inc.

Volkov, V. V. and D. I. Svergun (2003). "Uniqueness of ab initio shape determination in small-angle scattering." Journal of Applied Crystallography **36**: 860-864.

Walworth, N. C. and P. J. Novick (1987). "Purification and characterization of constitutive secretory vesicles from yeast." J Cell Biol **105**(1): 163-174.

Wang, X. H., K. Nakayama, et al. (1997). "MNN6, a member of the KRE2/MNT1 family, is the gene for mannosylphosphate transfer in Saccharomyces cerevisiae." J Biol Chem **272**(29): 18117-18124.

Williams, D. B. (2006). "Beyond lectins: the calnexin/calreticulin chaperone system of the endoplasmic reticulum." J Cell Sci **119**(Pt 4): 615-623.

Withers, S. G., W. W. Wakarchuk, et al. (2002). "One step closer to a sweet conclusion." Chem Biol **9**(12): 1270-1273.